POLITECNICO
MILANO 1863

SCUOLA DI INGEGNERIA INDUSTRIALE
E DELL'INFORMAZIONE

Bifurcation analysis of spontaneous flows in active nematic fluids

Tesi di Laurea Magistrale in
Mathematical Engineering - Ingegneria Matematica

Author: **Arsène Marzorati**

Student ID: 96378
Advisor: Prof. Stefano Turzi
Academic Year: 2021-22

Abstract

This thesis is the study of a degeneracy for a simple problem developed with an alternative model of active nematics. While the active matter field is still in development (§1), the classic models are not unanimous because of thermodynamics questions. An alternative approaches still based on liquid crystals, taking into account these problems, shows a very general and rich behavior even for the basic spontaneous-flow problem in a two-dimensional channel (§2). This bifurcation is generic and invariant with material changes (§3) and a study with Lyapunov-Schmidt reduction and symmetric considerations allows us to draw the independent branches which do not overlap (§4).

Keywords: Active nematics, Bifurcation, Lyapunov-Schmidt reduction, symmetries

Acknowledgment: I would like to thank my professor ,Prof.Stefano Turzi, for his support, his availability and his patience during the realization of this thesis.

Contents

Introduction

Active matter is a recent challenge for many fields. Its understanding could lead to the explanation of many historical and crucial problems such as the mechanisms of cell division and reproduction. In addition, this new field has promising applications in medical and industrial fields.
Several results and models have been developed, inspired by different areas of scientific research, but the similarities among the observations and outcomes show that is possible to put forth a comprehensive theory. However the complexity of the studied systems, due to their composition and the high number of degrees of freedom, make this task difficult. Based on nematic liquid crystal theory, some models succeed to describe well the experimental results. However, controlling every feature of these systems in the modeling is extremely difficult and some assumptions still need to be critically revised to improve the theory. For this reason, the research in active matter is more and more developed, dealing with new fields such as Machine Learning.

The thesis is organized as follows. In Chapter 1, a brief presentation of active matter physics will be discussed together with some possible applications of the theory. Then, in Chapter 2, the classic continuum theories of active matter based on the Eriksen-Leslie of liquid crystals will be presented. However, we will work with an alternative model developed in [17]. Justifying the use of this model, we will state some results, particularly the existence of spontaneous flow coming from a bifurcation. In Chapter 3, we will test the previous results against some changes in material parameters. In Chapter 4, we further analyze the bifurcation by means of the Lyapunov-Schmidt reduction. We illustrate the method with two examples before applying it to our model. Finally, in Chapter **??**, we will show that the system is invariant under a symmetry group, allowing us to state that the bifurcation diagram is generic.

1 | Active matter

In this chapter, a brief presentation of active matter will be done in §1.1. Some biological applications will be presented to emphasize the continuously growing interest in the field in §1.2.

1.1. Active matter: Description

Active matter is a recent research field of interest. As underlined in [11], "Production of peer-reviewed papers with 'active matter' in the title or abstract has increased from less than 10 per year two decades ago to almost 70" in 2015, and several international workshops have been held on the topic the same year.
This growing attractiveness is due to two main reasons. The first is its large spectrum of applications. These go from microscopic scale, with cells layers and colonies of bacteria, to macroscopic scale, for example fish schools and bird flocks (see Figure1.1), even passing by non-living systems such as collections of robots. This variety attracted scientists from several fields such as Biology, Mathematics, Physics, and others.
The second is the type of problems dealing with the theory. They concern classic physical quantities such as energy, movement, work, and fluctuations but out of thermodynamical equilibrium. In addition, the complexity of the systems makes the building of theory very challenging, to the extent that, nowadays, even machine learning is considered to find the model parameters able to fit the observations.

Figure 1.1: Example of bird flock (*source: Wikipedia*).

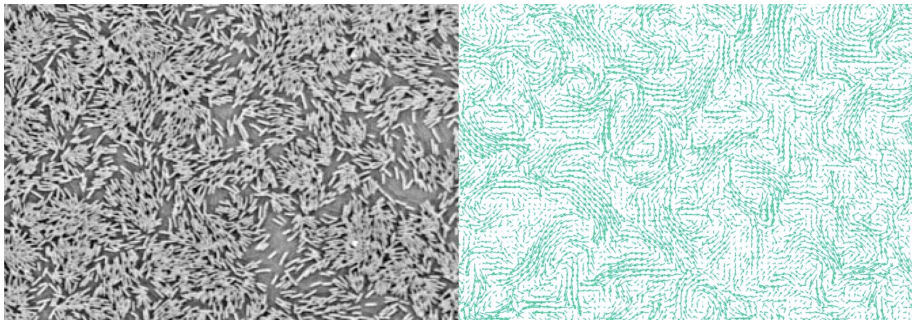

Figure 1.2: Collective motion in bacterial suspensions. At the right: Typical snapshot of the velocity field measured in a high-density cell suspension. (*source: Max Planck Institute for terrestrial Microbiology/Colin*).

Before explaining the challenges behind the modeling, a brief historical recap is in order. In the 1990s, Vicsek looked at the collective motion of bird and cytoskeleton components. He proposed a model inspired by Heinsberg's work on magnetic materials [18]. The success of his results made others study the subject, and in 1994 Toner developed a continuum model based on standard equations of hydrodynamics and obtained the same kind of results.
The field had to wait until the 2000s to have the first experimental results from Bausch with cytoskeleton components [14]. In 2014, Dogic, Bausch, and Marchetti began to formulate one of the first complete theoretical approaches for active liquid crystals [8].

But what exactly is called "active matter"? As underlined in [12], the living systems have the faculty to move, change their shape, and create their morphology. This can even

Figure 1.3: Explication of collective behavior of bird flock. Left image, low density the individuals have their own behavior, no collective movement. Right image, high density, the individuals tend to align with their neighbors creating a collective movement. (*source: Nature*)

be observed at the scale of the building elements of living systems: cells. Due to the large variety of the systems that can be referred to as "active matter", the definition can change with the subject. However, some similarities are observed. An active system is composed of self-driven units which can continuously interact with the medium they live in, particularly exchange energy with it. They can store this energy or transform it into mechanic one[4, 9]. This specificity results in another important property, the emergence of collective behavior differing from the individual one. Figure1.3 illustrates perfectly this result with bird flocks. In the case of a low density of individuals, each one has its own behavior (here random flight direction). When the density crosses a threshold, the individuals tend to align their own movement with one of their neighbors, causing this collective motion (see Figure1.1) and it can be observed the same effect at a microscopic scale (see Figure1.2).
For example, there is increasing evidence that this collective behavior is important for providing the cells with the ability to invade and occupy their surroundings.
Therefore, understanding the mechanism of this collective motion is highly relevant to natural systems across a wide range of length scales. This suggests that a general understanding of this principle rather than specific, i.e., relative to a length scale, could be a very powerful and useful theory.

However, modeling such a mechanism raises many challenges. First, the theory behind this system can be very different from the classic equilibrium models because these systems lack time-reversal symmetry. Indeed, energy is constantly transduced. In addition, they are always out of thermodynamic equilibrium. It is even difficult to identify the key parameters and degrees of freedom.

And indeed, it seems difficult to describe a set of general proprieties for active matter because of the large number of systems and also by their complexity. As emphasized in [9], for a living organism there are at least 300 cells and each one has a dynamical process depending on many variables. And this becomes more and more complex for multicellular eukaryotic organisms, for example in the animal world.

That creates new challenges for the mathematical modeling of these systems [3]. According to Dogic, active matter changed the ideas of what materials can do. Indeed, "by studying the spontaneous flows of microtubules and proteins confined in small, doughnut-shaped containers, it is hoped to lay the groundwork for a self-pumping fluid that could move molecules around in microfluidic devices similar to those that are becoming increasingly common in experimental biology, medicine, and industry."

In the next section, this aspect will be presented through different problems and applications that illustrate the interest in developing such a theory.

1.2. Applications

Why is active matter interesting? In this section, the development will be split into two parts. The first one will show that the mechanism of active systems is responsible for phenomena that are still difficult to explain for the scientific community. The second part will underline the possible improvements that could be done if the results of the theory are applied to some technologies.

1.2.1. Fundamental problems

As it has been underlined in§1.1, active matter involves many subjects because of the numerous scales where it appears. As it has already been described, the collective behavior or motion that can be observed with birds or fish in everyday life is a phenomenon due to the mechanism of active matter. Before his work, Vicsek underlined the nonexistence of theory to describe it. But he built a model to tackle also the same behavior with bacteria and cells.

According to [12], it is possible to describe a complex mechanism which is one of the

fundamentals to understand living beings. Indeed at the cell scale, the modeling of active matter relies on the cytoskeleton, a biopolymeric system (in other words a network of interlinking protein filaments) that controls the mechanical properties of the cells such as division and movement. The latter is formed by three types of filaments: Intermediate, microtubules, and actin filaments (or microfilaments). Whereas the mechanical contribution of the intermediate filaments is passive and takes place at large deformations and over long times, the microtubules and microfilaments are structurally polar and provide a directionality for active processes. They are fundamentally out of equilibrium, continuously hydrolyzing ATP (Adenosine Triphosphate) for actin filaments or GTP (Guanosine Triphosphate) for microtubules into ADP or GDP (Adenosine Diphosphate) and (Guanosine Diphosphate). This activity results in polymerization at one end and depolymerization at the other end. This process, called treadmilling, has an important role in cell motility (spontaneous movement) and cell signaling.
These filaments have another important characteristic: they can act as tracks to energy-transducing proteins called molecular motors, which can ride along them. The latter can be distinguished into three families: myosins moving on actin filaments, kinesins, and dyneins moving on microtubules.
As for the motors, they can move the cytoskeletal filaments if they are anchored on a substrate or a crosslinked structure such as a gel. Most of the mechanical properties of animal cells are controlled by a thin layer of the actomyosin meshwork (a few hundred nanometres to micrometers thick) called the cell cortex. It is a dense gel with a mesh size of a few tens of nanometres. At first sight, it can be considered a physical gel because the actin filaments are crosslinked by proteins having a finite bound time. The treadmilling phenomenon and the action of myosins, however, introduce fundamentally novel aspects to the system.

Furthermore, some important problems such as swimming bacteria could be described by the theory. And experimental works on active matter could provide a base for testing theories of non-equilibrium statistical physics[20]. But understanding active matter is not only the unlocking of complex mechanism explanations. Scientists can apply the results in many fields and technologies.

1.2.2. Applications in medicine and environment

In the development of technologies, one of the most widespread ideas is based on the analogy with nature. In other words to imitate how living entities accomplish the ex-

pected tasks. Why not copy a process that has evolved for thousands of years?
The utilization of microrobots is more and more developed because the small size allows the accomplishment of tasks that humans cannot perform. Contrary to previous methods, humans can have control of the robot's action. However, the performance of this technology is limited by the difficulties encountered by a unique robot in fluid flow (whether water or human blood). In this situation, active matter could play a key role to improve the performance of a collection of microrobots. Indeed, they can reproduce the movement of bacteria or cells which could be an asset. Two examples will illustrate this idea. The first is about the environment and wastewater treatment. The second is about biomedical technologies.

But first, the concept of swarm robotic. The idea is to apply collective behavior to robots. And then, control their movement and action. A swarm is composed of many individual units, each one having several degrees of freedom. When it is controlled as a whole, it forms an active system having a collective behavior. In this kind of system, the loss of a few units by technical problems or other factors does not impact the functions of the swarm. This robust behavior of the swarm is a clear advantage compared to a unique robot.

To generate the motion, i.e., force the robots to group in a swarm, there exist different methods each of which with pros and cons for [5].

Magnetic method: It is the most used control. It applies magnetic forces to the robots with coil systems or permanent magnets. This is done at distance allowing to work in confined and narrow spaces such as the human body. However, in bigger spaces, it becomes complicated to generate a strong magnetic field to control efficiently the swarm requiring more energy and complex design. For safety considerations, a short exposure for humans is not proven to be dangerous so far. Except for a very strong magnetic field ($\sim$ 10 T), in this case, the patient can feel some knock-on effects such as metallic tastes and dizziness. On the environmental scale, a long exposure can impact the living individuals and becomes problematic.

Electric method: In this case, the microrobots are controlled by the Coulomb force generated by an external electric field. The field polarizes the material and induces dipole within the microrobots. Then, interactions between dipoles generate the creation of the

swarm. Compared with the magnetic field, the electric field has similar advantages in working environments. However, for biosafety concerns, living cells can be damaged by the electrophoresis [1] and hydrogel polymerization caused by electric fields. The generation of the electric field has more problems to overcome. Generating electric fields in a large volume requires large electrodes, bringing design challenges about safety and efficiency.

Acoustic method: The microrobots are driven by the energy of the sound wave. Controlling the frequency and the phase, it is possible to design the acoustic pressure distribution in the medium and the microrobots move with respect to the pressure gradient and its geometrical shape. Unlike magnetic fields, the transmission of sound waves needs a material medium. It can bring benefits by designing unique transmission media for a better control effect. However, it can also lead to problems dealing with complex media, such as the human body. Acoustic control shares the same advantages in the working space and health risks as magnetic control, but the device is much lighter. The feature of microrobots controlled by acoustic waves does not have a strict limitation. This high adaptivity also helps the acoustic field cooperate with other fields.

Optic method: It is possible to control robots with light. In this case, they are made from light-responsive polymers or biological materials, this is a great advantage in terms of biosafety regarding the human body and environment. This method has high accuracy and the energy transfer efficiency is elevated if directly exposed to the source. However, the properties of the control are altered if the environment makes difficult the propagation of the light such as in complex environments, and the penetration ability of the light is lower than a magnetic field. In this case, optic fiber can be used to overcome these obstacles but the field is not yet mature enough and requires more research.

Chemical method: In this situation microrobots use the energy produced in chemical reactions to power their locomotion, functioning as a catalyst. They are active as long as the fuel reagents exist. This method is efficient for powering the microrobots. However, it is difficult to control the swarm behavior in real-time because it is difficult to adjust in live time the properties of the solution. Thus, additional fields, such as magnetic and acoustic, need to be applied in order to control collective behavior. In biomedical applications, the

[1] Electrophoresis is a general term that describes the migration and separation of charged particles (ions) under the influence of an electric field. *source: R.J. Fritsch, I. Krause, in Encyclopedia of Food Sciences and Nutrition (Second Edition), 2003.* This is problematic because the motion of proteins responsible for several mechanisms of the cell is influenced by this specific migration.

selection of the chemical reaction is vital to the system's performance. The reaction needs also to be safe inside the body, for example, using the biochemical reactions that exist inside the human body. In environmental application, however, potential pollution by microrobots is a matter of concern in selecting the proper reaction to power them.

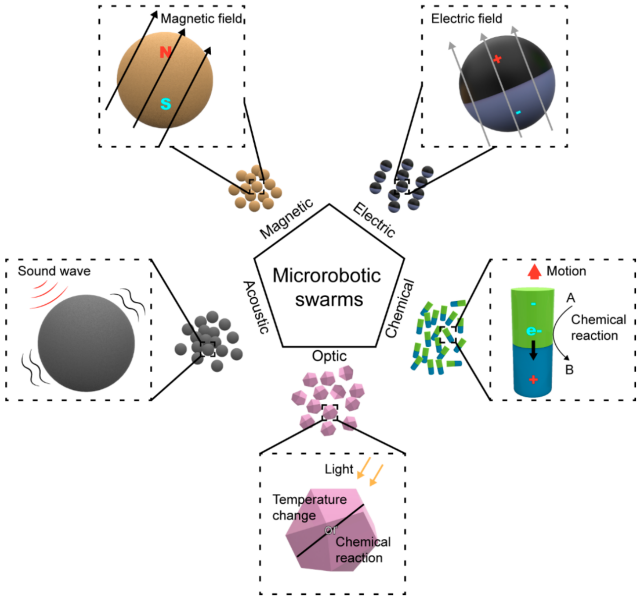

Figure 1.4: Example of bird flock (*source: Yulei Fu and al*).

Currently, the working environment of the microrobot swarms includes solid surface , liquid-air, liquid-liquid interfaces, and inside bulk liquid environment. These environments cover most of the applicational fields of microrobotic swarms.
However, the microrobotic swarms working in gaseous environments are not very studied whereas they can be very useful. In the biomedical field, they could be used for curing respiratory diseases. For the environment, the air pollution problem is another possible area of application.

Biomedicine technologies: In medicine especially in oncology, some classic treatments are particularly painful for the patient. A key solution is to target locally the tumor. The use of swarm robots could answer this need. For example, they can bring the proteins or the chemical drug required to kill the cancerous cells. For example, in Brachytherapy [2], it is needed to bring a radioactive source to destroy the tumor cells. With the swarm, it

[2]Brachytherapy is a type of internal radiation therapy in which seeds, ribbons, or capsules that contain a radiation source are placed in the body, in or near the tumor. Brachytherapy is a local treatment and treats only a specific part of the body. It is often used to treat cancers of the head and neck, breast, cervix, prostate, and eye. *source: National Cancer Institute*

becomes possible to bring the quantity needed close to the tumor and not use traditional radiotherapy which is dangerous for patients.
Another possibility is to use the swarm for improving the blood flow in order to dissolve a blood clot. And this avoids using pharmaceutic treatments which can bring second effects.
One last but not least example is the use of a swarm to remove harmful biofilms. For example, it has been used to destroy the membrane of bacteria and biofilms on medical and industrial equipment[5, 6].
Despite significant progress in the use of microswarms in biotechnologies, some challenges have still to be overcome. For example, the efficiency of the targeted therapy can be low. Indeed, the microrobots are seen as intruders and are attacked by the immune system. Even the control method has to be improved in order to overcome the obstacle for the microrobots in complex geometries.

Environment and wastewater treatment:
Different sources of pollution contribute to the shortage of water problem such as oil leakage industrial sewage and heavy metal pollution. Once again the control of this swarm is to destroy the polluted particles or filtrated them.
Microrobots are already used in this area but swarms have not been applied yet but could be a promising subfield of research allying active matter and robotics. However one major limit is the fact that they become themselves a source of pollution[5, 6].

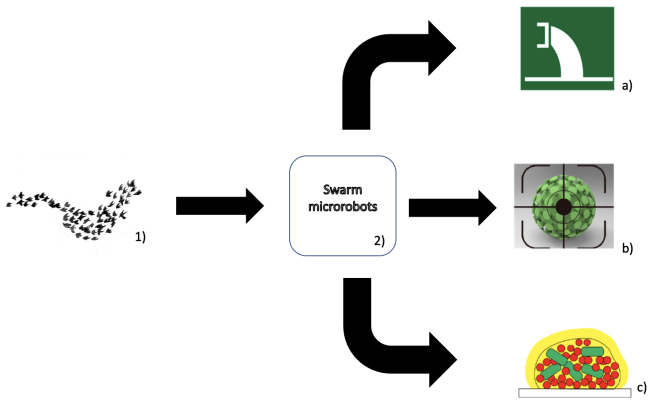

Figure 1.5: From collective behavior in nature (1) to swarm robotic (2). Possible application: a) waste water treatment, b) Target Therapy, c) Remove harmful biofilms.

2 | Model of active nematics

As was underlined in the previous chapter (1) and according to[4] "convergent strands of research focused on modeling bacterial swarms and on cytoskeletal dynamics have suggested that the collective behavior seen in both types of system can be described in the continuum limit by the same phenomenological, hydrodynamic model".
The complexity of the system has been dealt already in several works. And classically, continuum hydrodynamic models of active liquid crystals have been used to describe this dynamic of self-organizing systems such as bacterial swarms. A key prediction of such models is the existence of self-stabilizing states that spontaneously generate fluid flow in a quasi-one-dimensional channel.
After introducing a general background for the theory of active nematics in §2.2, the model used in this work will be presented in §2.3. The last part of the chapter, in §2.4, will focus on a quasi-one-dimensional example to describe a specific and benchmark case: "Spontaneous flow".

2.1. Notations

This section is a short recap of all the notations which will be found in the next sections.

- The material time derivative:
$$(\dot{\ }) = \frac{D}{Dt} = \frac{\partial}{\partial t} + \mathbf{v} \cdot \frac{\partial}{\partial x}.$$
- The nabla operator ∇ is used.

Because only Cartesian coordinates are considered in this work, it is defined as:

$$\nabla = \begin{pmatrix} \frac{\partial}{\partial x} \\ \frac{\partial}{\partial y} \\ \frac{\partial}{\partial z} \end{pmatrix}.$$

All the classic derivative operators can be expressed with it. We recall: div $= \nabla\cdot$,

$\Delta = \nabla \cdot \nabla$, rot $= \nabla \times$.

- We recall the dot product for second-rank tensors.

$$A \cdot B = \mathrm{tr}(B^T A).$$

- The tensor product between to second-rank tensors.

$$(A \otimes B)X = AXB^T.$$

- The codeformational derivative:

$$\mathbf{B}_e^{\nabla} := (\mathbf{B}_e)^{\cdot} - (\nabla \mathbf{v})\mathbf{B}_e - \mathbf{B}_e(\nabla \mathbf{v})^T.$$

2.2. Liquid crystals (LC) and active nematics

In this section, we will present the Eriksen-Leslie theory of liquid crystals and its extension to active nematics and we will follow [15].

2.2.1. LC: director, deformations and energy

As underlined in [3], a well-studied class of active matter such as elongated bacteria or filamentous particles can be simply generalized to a group of rod-shaped particles which have similitudes with nematic liquids. The latter describes elongated molecules with long-range orientational order. This consideration allows us to adapt the developed theory of liquid crystals for modeling active matter. The difference lies in the consideration of activity.

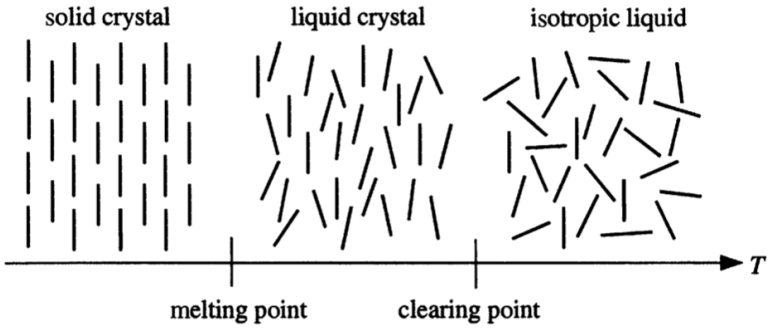

Figure 2.1: Difference in terms of ordering between, Crystal, Liquid Crystal and Liquid (*Source: "The Static and Dynamic Continuum Theory of Liquid Crystals"* [15])

Liquid crystals are anisotropic and non-Newtonian liquids. Often described as an intermediate state between liquid and crystal, these mesophases can flow like a liquid but they have some anisotropic physical properties (i.e., depending on the direction) as crystals. The nematic liquid crystals exhibit a preferred direction along which the axis of each constituent tends to align (see Figure2.2). This direction is called the anisotropic axis or director and will be denoted with **n**. There is no correlation between the center of mass of the molecules, i.e., they can freely translate while being aligned parallel to one another on average. In addition, we consider nematic particles, that is elongated particles possessing head-tail symmetry, in a uniaxial phase, where there is only one preferred anisotropic axis.
Developed in the 1920s, the hydrodynamic theory has been put forward by Leslie and Eriksen in the 1960's. They based their work on the extension of the static equilibrium theory developed by Frank, which introduces the so-called Frank-Oseen elastic for the director distortions.

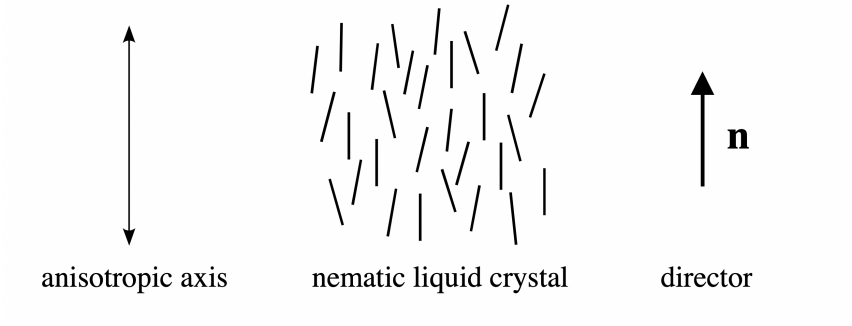

Figure 2.2: Ordering in nematic liquids crystals (*Source: "The Static and Dynamic Continuum Theory of Liquid Crystals"* [15])

This energy accounts for the possible distortions of the director. There exist three types of distortions: Splay, Twist, and Bend (see Figure2.3).

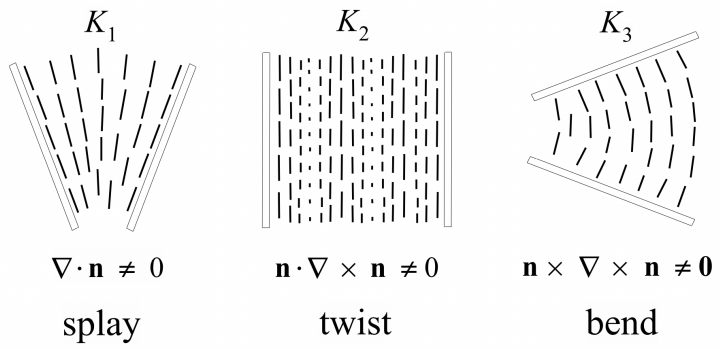

Figure 2.3: Possibles distortions of nematics (*Source: "The Static and Dynamic Continuum Theory of Liquid Crystals"* [15])

In the static case, the director $\mathbf{n}$ tends to align in a direction minimizing this energy. The latter is assumed to be invariant with respect to the symmetry $\mathbf{n} \mapsto -\mathbf{n}$, called nematic symmetry, quadratic in the gradient of $\mathbf{n}$, and frame indifferent[1]. It is written as follows[15],

$$w_F(\mathbf{n}, \nabla\mathbf{n}) = \frac{1}{2}\Big(K_1(\nabla \cdot \mathbf{n})^2 + K_2(\mathbf{n} \cdot \nabla \times \mathbf{n})^2 + K_3(\mathbf{n} \times \nabla \times \mathbf{n})^2$$

$$(K_2 + K_4)\nabla \cdot [(\mathbf{n} \cdot \nabla)\mathbf{n} - (\nabla \cdot \mathbf{n})\mathbf{n}]\Big), \tag{2.1}$$

where K_i are the Frank constants, related with a specific distortion as it can be seen on Figure2.3. The "one constant approximation" consisting in taking $K = K_1 = K_2 = K_3$ and $K_4 = 0$, reduces equation (2.1) to

$$w_F = \frac{1}{2}K||\nabla\mathbf{n}||^2. \tag{2.2}$$

We will make this simplification in the rest of the thesis.
The continuum description of Liquid Crystals is built similarly to polar fluids. The spatial description of the instantaneous motion of a fluid with microstructure uses two independent vector fields: the velocity $\mathbf{v}(x,t)$ and an axial vector $\mathbf{w}(x,t)$ which is the local angular velocity of the director $\mathbf{n}$ (for polar fluids it is the angular velocity of the particle). This is because $\mathbf{n}$ is an independent degree of freedom and it is not materially transported by

[1]The constitutive laws governing the internal conditions of a physical system and the interactions between its parts should not depend on whatever external frame of reference is used to describe them.

the flow.
In the classic continuum theory, only the velocity field is independent and the angular velocity $\hat{\mathbf{w}}$ is related to its curl. It is a measure of the average rotation of the fluid over a neighborhood of the director and is interpreted as the regional angular velocity.Then a relative angular velocity is defined as the difference between the two: ω.
Therefore we have,

$$\hat{\mathbf{w}} = \frac{1}{2}\nabla \times \mathbf{v}, \tag{2.3}$$

$$\omega = \mathbf{w} - \hat{\mathbf{w}}, \tag{2.4}$$

and the following properties of the director $\mathbf{n} \cdot \mathbf{n} = 1$ and $\mathbf{w} \times \mathbf{n} = \dot{\mathbf{n}}$.

The rate of strain tensor $\mathbf{D}$ and the vorticity tensor $\mathbf{W}$ are defined as[2]:

$$\mathbf{D} = \frac{1}{2}\Big(\nabla\mathbf{v} + (\nabla\mathbf{v})^T\Big), \quad \mathbf{W} = \frac{1}{2}\Big(\nabla\mathbf{v} - (\nabla\mathbf{v})^T\Big). \tag{2.5}$$

The co-rotational time flux of the director is defined as

$$\mathring{\mathbf{n}} = \omega \times \mathbf{n} = \dot{\mathbf{n}} - \mathbf{W}\mathbf{n}. \tag{2.6}$$

All the quantities, $\mathbf{n}$, $\mathbf{D}$, and $\mathring{\mathbf{n}}$ are material frame-indifferent. In addition, isothermal conditions and incompressibility are assumed whereas thermal effects are ignored.

2.2.2. LC: Dynamic and Eriksen-Leslie theory

As in classic continuum theory, conservation laws for mass (2.7), linear (2.8) and angular (2.9) momentum must hold,

$$\frac{D}{Dt}\int_V \rho \, dV = 0, \tag{2.7}$$

$$\frac{D}{Dt}\int_V \rho\mathbf{v} \, dV = \int_V \rho\mathbf{f} \, dV + \int_S \mathbf{t} \, dS, \tag{2.8}$$

$$\frac{D}{Dt}\int_V \rho(\mathbf{x} \times \mathbf{v}) \, dV = \int_V \rho(\mathbf{x} \times \mathbf{f} + \mathbf{K}) \, dV + \int_S (\mathbf{x} \times \mathbf{t} + \mathbf{l}) \, dS. \tag{2.9}$$

- ρ is the density, $\mathbf{x}$ is the position vector, $\mathbf{v}$ is the velocity.

[2]By definition, this tensor is the unique tensor satisfying for any vector $\mathbf{u}$, $\mathbf{W}\mathbf{u} = \hat{\mathbf{w}} \times \mathbf{u}$.

- $\mathbf{f}$ is the external body force per unit mass, $\mathbf{K}$ is the external body moment per unit mass.
- $\mathbf{t}$ is the surface force per unit area, $\mathbf{l}$ is the surface moment per unit area.

The director terms are incorporated in the rate of work equation, so we have

$$\int_V \rho(\mathbf{f}\cdot\mathbf{v}+\mathbf{K}\cdot\mathbf{w})\,dV+\int_S(\mathbf{t}\cdot\mathbf{v}+\mathbf{l}\cdot\mathbf{w})\,dS=\frac{D}{Dt}\int_V(\frac{1}{2}\rho\mathbf{v}\cdot\mathbf{v}+w_F)\,dV+\int_V\mathscr{D}_{EL}\,dV. \tag{2.10}$$

$\mathscr{D}_{EL}$ is the viscous dissipation rate per unit volume and it is assumed non-negative. The following relations between stress tensor ($\mathbf{T}$) and surface force ($\mathbf{t}$), and, the couple stress tensor ($\mathbf{L}$) and the surface ($\mathbf{l}$) moment can be proved: $\mathbf{t}=\mathbf{T}\mathbf{v}$ and $\mathbf{l}=\mathbf{L}\mathbf{v}$. Then, exploiting the previous balance laws (equations (2.7)-(2.9)), we derive

$$\mathbf{T}=-p\mathbf{I}-(\nabla\mathbf{n})^T\frac{\partial w_F}{\partial\nabla\mathbf{n}}+\tilde{\mathbf{T}}, \tag{2.11}$$

$$\mathbf{L}=\mathbf{n}\times\frac{\partial w_F}{\partial\nabla\mathbf{n}}+\tilde{\mathbf{L}}. \tag{2.12}$$

- p is an arbitrary pressure coming from incompressibility.
- $\tilde{\mathbf{T}}$ and $\tilde{\mathbf{L}}$ are possible dynamic contributions. The first is called viscous stress.

Under the assumption that $\tilde{\mathbf{L}}$ does not depend on the gradients of $\mathbf{w}$, the dissipation inequality leads to $\tilde{\mathbf{L}}=0$, reducing equation (2.10) to

$$\tilde{\mathbf{T}}\cdot\nabla\mathbf{v}-\mathbf{W}\cdot\tilde{\mathbf{T}}=\mathscr{D}_{EL}\geq 0. \tag{2.13}$$

It is supposed that $\tilde{\mathbf{T}}$ is a function of $\mathbf{n}$, $\mathbf{w}$, and $\nabla\mathbf{v}$ which is equivalent, under assumptions and properties of $\mathbf{w}$, to be a function of $\mathbf{n}$, $\mathring{\mathbf{n}}$, and $\mathbf{D}$. In addition the material frame-indifference requires $\tilde{\mathbf{T}}$ to be an hemitropic function (invariant under rotation) of these variables and symmetries imply to be an isotropic function of them. Leading to the Leslie formula

$$\tilde{\mathbf{T}}=\alpha_1\big(\mathbf{n}\cdot\mathbf{D}\mathbf{n}\big)\,\mathbf{n}\otimes\mathbf{n}+\alpha_2\,\mathring{\mathbf{n}}\otimes\mathbf{n}+\alpha_3\,\mathbf{n}\otimes\mathring{\mathbf{n}}+\alpha_4\,\mathbf{D}+\alpha_5\,\mathbf{D}\mathbf{n}\otimes\mathbf{n}+\alpha_6\,\mathbf{n}\otimes\mathbf{D}\mathbf{n}. \tag{2.14}$$

The coefficients α_i are called Leslie viscosity coefficients. The Parodi relation gives

$$\alpha_6 - \alpha_5 = \alpha_2 + \alpha_3$$

reducing the number of independent viscosities from six to five. The viscous dissipation can be written as

$$\mathscr{D}_{EL} = \alpha_1 \, (\mathbf{n} \cdot \mathbf{Dn})^2 + 2\gamma_2 \mathring{\mathbf{n}} \cdot \mathbf{Dn} + \alpha_4 \, \mathbf{D} \cdot \mathbf{D} + (\alpha_5 + \alpha_6) \mathbf{Dn} \cdot \mathbf{Dn} + \gamma_1 \, \mathring{\mathbf{n}} \cdot \mathring{\mathbf{n}} \geq 0. \quad (2.15)$$

Setting $\gamma_1 = \alpha_3 - \alpha_2$ and $\gamma_2 = \alpha_6 - \alpha_5$. The previous relation constrains the viscosity coefficients to

$$\begin{cases} \gamma_1 \geq 0, \\ \alpha_4 \geq 0, \\ 2\alpha_4 + \alpha_5 + \alpha_6 \geq 0, \\ 2\alpha_1 + 3\alpha_4 + 2\alpha_5 + 2\alpha_6 \geq 0, \\ 4\gamma_1(2\alpha_4 + \alpha_5 + \alpha_6) \geq (\alpha_2 + \alpha_3 + \gamma_2)^2. \end{cases}$$

It can be distinguished two kinds of flow for nematics with the coefficients α_2 and α_3,

$$\text{Flow aligning} : \alpha_2 \alpha_3 > 0 \text{ and } \alpha_2 < \alpha_3 < 0 \quad (2.16)$$

$$\text{Tumbling} : \alpha_2 \alpha_3 < 0 \quad (2.17)$$

In the first, the director tends to a steady-state whereas in the second, it is not able to reach a fixed state making the particles rotate inside the flow and leading to defect formation.

Finally, the Eriksen-Leslie equations can be stated.
Director constraint,

$$||\mathbf{n}|| = 1, \quad (2.18)$$

Incompressibility,

$$\nabla \cdot \mathbf{v} = 0, \quad (2.19)$$

Balance of linear momentum,

$$\rho \dot{\mathbf{v}} = \rho \mathbf{f} - \nabla(p + w_F) - \big(\nabla \mathbf{n}\big)^T (\gamma_1 \mathring{\mathbf{n}} + \gamma_2 \mathbf{Dn}) + \big(\nabla \mathbf{n}\big)^T \mathbf{K}_G + \frac{\partial \tilde{\mathbf{T}}}{\partial \mathbf{x}}, \quad (2.20)$$

Balance of angular momentum,

$$\nabla\Big(\frac{\partial w_F}{\partial \nabla \mathbf{n}}\Big) - \frac{\partial w_F}{\partial \mathbf{n}} + \gamma_1 \mathring{\mathbf{n}} + \gamma_2\, \mathbf{D}\mathbf{n} + \mathbf{K}_G = \lambda \mathbf{n}, \tag{2.21}$$

with $\mathbf{K}_G$ is the generalized body force, related to the external body moment $\mathbf{K}$ through the following relation: $\rho\mathbf{K} = \mathbf{n} \times \mathbf{K}_G$. λ is a Lagrange multiplier due to the director constraint. There are eight equations for eight unknowns (three components of $\mathbf{v}$, three components of $\mathbf{n}$, the pressure p, and λ).
For further computations, we state the complete Cauchy stress tensor, in the compressible case, in the EL theory,

$$\begin{aligned}\mathbf{T}_{EL} = &- p_{iso}\mathbf{I} + \alpha_1\big(\mathbf{n}\cdot\mathbf{D}\mathbf{n}\big)\,\mathbf{n}\otimes\mathbf{n} + \alpha_2\,\mathring{\mathbf{n}}\otimes\mathbf{n} + \alpha_3\,\mathbf{n}\otimes\mathring{\mathbf{n}} + \alpha_4\,\mathbf{D} + \alpha_5\,\mathbf{D}\mathbf{n}\otimes\mathbf{n} \\ &+ \alpha_6\,\mathbf{n}\otimes\mathbf{D}\mathbf{n} + \alpha_7[(\mathrm{tr}D)(\mathbf{n}\otimes\mathbf{n}) + (\mathbf{n}\cdot\mathbf{D}\mathbf{n})\mathbf{I}] + \alpha_8(\mathrm{tr}D)\mathbf{I} - (\nabla\mathbf{n})^T\frac{\partial w_F}{\partial\nabla\mathbf{n}}.\end{aligned} \tag{2.22}$$

2.2.3. Active nematics: classic description

To describe active nematic, the previous theory is usually extended to include the notion of active stress. In several works [3, 4, 9], activity is an explicitly added piece to the general stress tensor. This is strongly related to the director, in other words, to the local structure of the molecules. It usually takes one of two forms

$$\mathbf{T}_\zeta = \zeta\mathbf{n}\otimes\mathbf{n}, \quad \mathbf{T}_\zeta = \zeta\mathbf{Q} = \zeta\frac{d}{d-1}q(\mathbf{n}\otimes\mathbf{n} - \mathbf{I}/d),$$

where $\mathbf{Q}$ is called the nematic order parameter tensor, d is the dimension of the space and q is the magnitude of the order. It is a traceless tensor.

However, this is not universally accepted for several reasons. For example, it is not compatible with irreversible thermodynamics [1, 16]. Indeed, active terms are irreversible which means under reversal time they do not change sign. Whereas, in the definitions of the previous $\mathbf{T}_\zeta$, the production of entropy is $\mathbf{T}_\zeta\cdot\nabla\mathbf{u} = \zeta\mathbf{Q}\cdot\nabla\mathbf{u}$. The quantity $\nabla\mathbf{u}$, being reversible, changes of sign requiring the same change for the scalar ζ under time reversal. Which is impossible for a scalar.
Another problem is the chemical power expended by the system vanishes when $\mathbf{v} = 0$. Indeed, the internal power $\mathbf{\Pi}_{int} = -\mathbf{T}\cdot\nabla\mathbf{v}$. Whereas it is expected that the power exerted by the active term does not vanish even in absence of any macroscopic flow. It is difficult to differentiate active and passive contributions when $\mathbf{T}_\zeta$ is used.

In the thesis, we will explore the consequences of an alternative model described in [17], where activity is introduced as a remodeling generalized force. Particularly, we will focus on the fact that standard analysis of polar theories reveals a single instability mode where no net flow is observed for no-slip boundary conditions. By contrast, numerical studies [10] show two modes of instability. One with positive activity ($\zeta > 0$) and flow aligning (equation (2.16)) and another one with negative activity and tumbling (equation (2.17)).

2.3. Active Model with material relaxation

The model presented in this section has been developed in [17] to extend and overcome some issues present in the standard active models. The reader is invited to look at the article for deeper justifications. Here, we will recall the principal considerations and equations while we will detail some computations in Appendix §7.1.

2.3.1. Theoretical model

The first key idea is to split the degrees of freedom associated with elastic deformations (reversible and conserves energy, described through $\mathbf{F}_e$) and ones related to the material relaxation and reorganization (irreversible, described through $\mathbf{G}$). The deformation gradient is decomposed as follows $\mathbf{F} = \mathbf{F}_e\mathbf{G}$ called Kröner-Lee-Rodriguez decomposition and for convenience the inverse relaxing strain $\mathbf{H} = (\mathbf{G}^T\mathbf{G})^{-1}$. The *effective* left-Cauchy-Green deformation tensor can be written as

$$\mathbf{B}_e = \mathbf{F}_e\mathbf{F}_e^T = \mathbf{F}\mathbf{G}^{-1}\mathbf{G}^T\mathbf{F}^T = \mathbf{F}\mathbf{H}\mathbf{F}^T. \tag{2.23}$$

Unlike most hydrodynamic theories of active nematic (see §2.2) we do not use the ordering tensor $\mathbf{Q}$ but the uniaxial and unit determinant *shape tensor*, coming from the theory of nematic elastomers,

$$\mathbf{\Psi}(\rho, \mathbf{n}) = a(\rho)^2(\mathbf{n} \otimes \mathbf{n}) + a(\rho)^{-1}(\mathbf{I} - \mathbf{n} \otimes \mathbf{n}). \tag{2.24}$$

- $\mathbf{n}$ is the preferred direction, the shape tensor represents the volume-preserving uniaxial stretch along it. As $\det(\mathbf{\Psi}) = 1$, the growth is not taken into account in the model.

- $a(\rho)$ is the shape parameter, giving the amount of spontaneous elongation along the preferred direction in a uniaxially ordered phase. The shape tensor is spherical, prolate or oblate for, respectively, $a(\rho) = 1$, $a(\rho) > 1$, or $a(\rho) < 1$.
- $\mathbf{I}$ is the identity tensor, ρ is the density.

The free-energy density per unit of mass is considered

$$\sigma(\rho, \mathbf{B}_e, \mathbf{n}, \nabla\mathbf{n}) = \sigma_0(\rho) + \frac{1}{2}\mu[\mathrm{tr}(\mathbf{\Psi}^{-1}\mathbf{B}_e - \mathbf{I}) - \log(\det(\mathbf{\Psi}^{-1}\mathbf{B}_e))] + \sigma_F(\rho, \mathbf{n}, \nabla\mathbf{n}), \quad (2.25)$$

- $\rho\mu$ is the shear modulus, $\sigma_0(\rho)$ models the compressibility and is not affected by stress relaxation.
- $\sigma_F(\rho, \mathbf{n}\nabla\mathbf{n})$ is the Oseen-Frank potential of liquid crystals [15] that favors the alignment of the director field $\mathbf{n}$, we have $w_F(\mathbf{n}, \nabla\mathbf{n}) = \rho\sigma_F$.

Now, we try to express the energy loss due to an irreversible process (entropy production) denoted with $\mathscr{D}$, a generalization of the viscous dissipation rate (see (2.15)) of the Eriksen-Leslie theory. Assuming an isothermal process and considering an arbitrary region $\mathscr{P}_t$ convecting with the body, the temporal increase in kinetic and free energies, respectively $\dot{K}$ and $\dot{\mathscr{F}}$ is required to be less than or equal to the power expended on the region by the external forces, denoted with W^{ext}.

$$\mathscr{D} := W^{ext} - \dot{K} - \dot{\mathscr{F}} \geq 0, \quad (2.26)$$

With

$$W^{ext} := \int_{\mathscr{P}_t} \mathbf{b}\cdot\mathbf{v}dv + \int_{\partial\mathscr{P}_t} \mathbf{t}_\nu\cdot\mathbf{v}da + \int_{\mathscr{P}_t} \mathbf{g}\cdot\dot{\mathbf{n}}dv + \int_{\partial\mathscr{P}_t} \mathbf{m}_\nu\cdot\dot{\mathbf{n}}da + \int_{\mathscr{P}_t} \mathbf{T}_a\cdot\mathbf{B}_e^{\nabla}dv,$$
$$K + \mathscr{F} := \int_{\mathscr{P}_t} \Big(\frac{1}{2}\rho\mathbf{v}^2 + \rho\sigma(\rho, \mathbf{B}_e, \mathbf{n}, \nabla\mathbf{n})\Big)dv.$$

All the quantities have already been introduced in §2.2.2 (see equation (2.10)) and they are redefined in Appendix §7.1.1 by comparison, except for the last and new term in the definition of W^{ext}. $\mathbf{T}_a$ is a second-rank tensor representing an external remodeling force that competes with the natural microscopic reorganization of the body. It has to be underlined that this tensor is conjugate to the remodeling velocity field $\mathbf{B}_e^{\nabla}$ contrary to the classic active stress conjugated with the gradient of velocity (see §2.2.3). $\mathbf{B}_e^{\nabla}$ has the following properties: (i) it is frame invariant, (ii) it vanishes when the deformation is purely elastic (no evolution of the natural configuration) (iii) and it comes out naturally

when studying the passive remodeling.

This leads to the following formula for the dissipation (for detailed computations see [17])

$$\begin{aligned}\mathscr{D} = &\int_{\mathscr{P}_t} (\mathbf{b} - \rho\dot{\mathbf{v}} + \mathrm{div}\mathbf{T}) \cdot \mathbf{v} dv \; + \int_{\partial\mathscr{P}_t} (\mathbf{t}_\nu - \mathbf{T}\nu) \cdot \mathbf{v} da \; + \int_{\mathscr{P}_t} (\mathbf{g} - \mathbf{h}) \cdot \dot{\mathbf{n}} dv \\ &+ \int_{\partial\mathscr{P}_t} \left[\mathbf{m}_\nu - (\rho \frac{\partial\sigma}{\partial\nabla\mathbf{n}})\nu\right] \cdot \dot{\mathbf{n}} da \; + \int_{\mathscr{P}_t} (\mathbf{T}_a - \rho\frac{\partial\sigma}{\partial\mathbf{B}_e}) \cdot \mathbf{B}_e^{\nabla} dv, \end{aligned} \tag{2.27}$$

where two important quantities, the Cauchy stress tensor, and the molecular field, are found to be

$$\mathbf{T} := -\rho^2 \frac{\partial\sigma}{\partial\rho}\mathbf{I} + 2\rho\frac{\partial\sigma}{\partial\mathbf{B}_e}\mathbf{B}_e - \rho(\nabla\mathbf{n})^T \frac{\partial\sigma}{\partial\nabla\mathbf{n}}, \tag{2.28}$$

$$\mathbf{h} := \rho\frac{\partial\sigma}{\partial\mathbf{n}} - \mathrm{div}\Big(\rho\frac{\partial\sigma}{\partial\nabla\mathbf{n}}\Big). \tag{2.29}$$

2.3.2. Equations and relaxation dynamic

According to the model, the material response is elastic with respect to the natural configuration. Energy is dissipated only when there is a microscopic reorganization. In equation (2.27) only the term depending $\mathbf{B}_e^{\nabla}$ yields a non-zero contribution. As $\mathscr{P}_t$ is arbitrary, we can get the following equations.
The classic balance of momentum and the corresponding boundary conditions are

$$\rho\dot{\mathbf{v}} = \mathbf{b} + div(\mathbf{T}), \tag{2.30}$$

$$\mathbf{t}_{(\nu)} = \mathbf{T}\nu. \tag{2.31}$$

Since $\dot{\mathbf{n}} = \mathbf{w} \times \mathbf{n}$, we have,

$$(\mathbf{g} - \mathbf{h}) \cdot \dot{\mathbf{n}} = (\mathbf{g} - \mathbf{h}) \cdot \mathbf{w} \times \mathbf{n} = \mathbf{w} \cdot \mathbf{n} \times (\mathbf{g} - \mathbf{h}).$$

Therefore, the microstructure satisfies the following equation and the corresponding boundary conditions

$$\mathbf{n} \times (\mathbf{g} - \mathbf{h}) = 0, \tag{2.32}$$

$$\mathbf{n} \times \mathbf{m}_{(\nu)} = \mathbf{n} \times \Big(\rho\frac{\partial\sigma}{\partial\nabla\mathbf{n}}\Big)\nu. \tag{2.33}$$

Finally, substituting all the equations (2.30)-(2.33) into equation (2.27), the positive

dissipation is imposed through (see Appendix §7.1.2 for a detailed computation)

$$(\mathbf{T}_a - \rho\frac{\partial\sigma}{\partial\mathbf{B}_e}) \cdot \mathbf{B}_e^{\nabla} = (\mathbf{T}_a - \frac{\rho\mu}{2}(\mathbf{\Psi^{-1}} - \mathbf{B}_e^{-1})) \cdot \mathbf{B}_e^{\nabla} \geq 0. \tag{2.34}$$

According to [16, 17], it is customary, when considering irreversible processes near equilibrium, to interpret the dissipation as the product of "fluxes" and "forces". Assuming a linear coupling between them and imposing symmetric constraint, we state that the evolution of the microscopic remodeling is governed by the following "gradient-flow" equation,

$$\mathbb{D}(\mathbf{B}_e^{\nabla}) + \rho\frac{\partial\sigma}{\partial\mathbf{B}_e} = \mathbf{T}_a. \tag{2.35}$$

where $\mathbb{D}$ is a symmetric positive definite fourth-rank tensor called the dissipation tensor. Substituting equation (2.35) into equation(2.28), we get,

$$\mathbf{T} := -\rho^2\frac{\partial\sigma}{\partial\rho}\mathbf{I} + 2[\mathbf{T}_a - \mathbb{D}(\mathbf{B}_e^{\nabla})]\mathbf{B}_e - \rho(\nabla\mathbf{n})^T\frac{\partial\sigma}{\partial\nabla\mathbf{n}}, \tag{2.36}$$

The equation (2.36) shows an active contribution to the stress tensor, $2\mathbf{T}_a\mathbf{B}_e$, which, however, depends on $\mathbf{B}_e$.
Before going further into the equations, we will focus on the form of $\mathbb{D}$. We can assume that it shares the uniaxial symmetry of the shape tensor $\mathbf{\Psi}$. As explained in [16], the most general matrix representation of a symmetric fourth-rank tensor that is transversely isotropic about $\mathbf{n}$ has five independent parameters. This tensor is an automorphism of the space of symmetric second-rank tensors which is defined on the following basis,

$$\mathbf{E}_1 = \frac{1}{\sqrt{2}}(\mathbf{e}_2 \otimes \mathbf{n} + \mathbf{n} \otimes \mathbf{e}_2), \qquad \mathbf{E}_2 = \frac{1}{\sqrt{2}}(\mathbf{e}_1 \otimes \mathbf{n} + \mathbf{n} \otimes \mathbf{e}_1), \tag{2.37a}$$

$$\mathbf{E}_3 = \frac{1}{\sqrt{2}}(\mathbf{e}_1 \otimes \mathbf{e}_2 + \mathbf{e}_2 \otimes \mathbf{e}_1), \qquad \mathbf{E}_4 = \frac{1}{\sqrt{2}}(\mathbf{e}_1 \otimes \mathbf{e}_1 - \mathbf{e}_2 \otimes \mathbf{e}_2), \tag{2.37b}$$

$$\mathbf{E}_5 = \sqrt{\frac{3}{2}}(\mathbf{n} \otimes \mathbf{n} + \mathbf{I}), \qquad \mathbf{E}_6 = \frac{1}{\sqrt{3}}\mathbf{I}. \tag{2.37c}$$

which is built with the orthonormal basis $(\mathbf{e}_1, \mathbf{e}_2, \mathbf{n})$ of $\mathbb{R}^3$. The basis $\{\mathbf{E}_i\}$ is orthonormal with respect to the classic dot product between second-rank tensors (see §2.1).
From acoustic experiments [17], we can express the dissipation tensor as,

$$\mathbb{D} = (\mathbf{\Psi}^{-1} \otimes \mathbf{\Psi}^{-1})\mathbb{T}. \tag{2.38}$$

The tensor $\mathbb{T}$ should be compatible with the uniaxial symmetry about $\mathbf{n}$, but it is not symmetric in general with respect to the classic dot product between second-rank tensors. Yet, it is symmetric with respect to the following scalar product,

$$\langle A, B\rangle = A \cdot (\mathbf{\Psi}^{-1} \otimes \mathbf{\Psi}^{-1})B = A \cdot \mathbf{\Psi}^{-1} B \mathbf{\Psi}^{-1}. \tag{2.39}$$

We also defined the corresponding outer product

$$(A \boxtimes B)X = A\langle B, X\rangle. \tag{2.40}$$

We derive a orthonormal basis with respect to the previous scalar product

$$\mathbf{L}_1 = \sqrt{a(\rho)}\mathbf{E}_1, \qquad \mathbf{L}_2 = \sqrt{a(\rho)}\mathbf{E}_2, \tag{2.41a}$$

$$\mathbf{L}_3 = a(\rho)^{-1}\mathbf{E}_3, \qquad \mathbf{L}_4 = a(\rho)^{-1}\mathbf{E}_4, \tag{2.41b}$$

$$\mathbf{L}_5 = \sqrt{\frac{2}{3}}(a(\rho)^2 \mathbf{n} \otimes \mathbf{n} - \frac{1}{2a(\rho)}(\mathbf{I} - \mathbf{n} \otimes \mathbf{n})), \qquad \mathbf{L}_6 = \frac{1}{\sqrt{3}}\mathbf{\Psi}. \tag{2.41c}$$

And we can get,

$$\begin{aligned}\mathbb{T} =& \tau_1(\mathbf{L}_1 \boxtimes \mathbf{L}_1 + \mathbf{L}_2 \boxtimes \mathbf{L}_2) + \tau_2(\mathbf{L}_3 \boxtimes \mathbf{L}_3 + \mathbf{L}_4 \boxtimes \mathbf{L}_4) + (\tau_s + \tau_d \cos(2\Theta))(\mathbf{L}_5 \boxtimes \mathbf{L}_5) \\ &+ (\tau_s - \tau_d \cos(2\Theta))(\mathbf{L}_6 \boxtimes \mathbf{L}_6) + \tau_d \sin(2\Theta)(\mathbf{L}_5 \boxtimes \mathbf{L}_6 + \mathbf{L}_6 \boxtimes \mathbf{L}_5).\end{aligned} \tag{2.42}$$

with $\tau_s = \frac{1}{2}(\tau_3 + \tau_4)$ and $\tau_s = \frac{1}{2}(\tau_3 - \tau_4)$. Θ is an additional parameter of the model which can be interpreted as the angle between the eigenspaces associated with τ_3 and $\mathbf{L}_5$ [16]. So we get the five parameters of the tensor $\mathbb{D}$. It is positive definite if and only if $\mathbb{T}$ is positive definite, requiring the positivity of the four relaxation times $\tau_i > 0$. That is always true.

2.3.3. Active fluid approximation

From now, the following assumptions are stated concerning only small effective deformations. To do so, two-time scales are defined.
The characteristic time for macroscopic deformation is defined as

$$\tau_{def} = ||\nabla \mathbf{v}||^{-1}. \tag{2.43}$$

The second characteristic time is related to material remodeling, determining the time rate at which $\mathbf{B}_e$ reaches equilibrium

$$\tau_{re} = 2||\mathbb{D}||/(\rho\mu). \tag{2.44}$$

We consider that

- $\tau_{re} \ll \tau_{def}$: Reorganization is much faster than deformation. The problem is reduced to purely hydrodynamic theory.
- It is assumed that the active term only introduces a small perturbation of the passive equilibrium value ($\mathbf{\Psi}$) of the effective strain tensor: $\mathbf{B}_e = \mathbf{\Psi} + \mathbf{B}_1$ with $||\mathbf{B}_1|| = O(\epsilon)$.
- $\mathbf{T}_a$ is the active tensor, here it will be taken as $\mathbf{T}_a = -\frac{1}{2}\rho\mu\zeta\mathbf{I}$.
- $\mathbb{D}$ is a fourth-rank tensor with major symmetries related to relaxation times (see §2.3.2 for further details). Here it is taken as $\mathbb{D} = \frac{1}{2}\rho\mu\tau\mathbb{I}$. $\mathbb{I}$ is the fourth-rank identity tensor. Compared to §2.3.2, it is an important simplification, we consider only one relaxation time.

The two hypotheses about the tensors $\mathbf{T}_a$ and $\mathbb{D}$ will be discussed in the next chapter (see Chapter 3).
The main contribution of $\mathbf{B}_e$) to the stress tensor comes from the codeformational derivative of the shape tensor,

$$\begin{aligned}\mathbf{\Psi}^{\nabla} =& \frac{\rho a'(\rho)}{a(\rho)^2}(\mathrm{tr}\mathbf{D})\{\mathbf{I} - [1 + 2a(\rho)^3](\mathbf{n}\otimes\mathbf{n})\} + [a(\rho)^2 - a(\rho)^{-1}](\mathring{\mathbf{n}}\otimes\mathbf{n} \\ &+ \mathbf{n}\otimes\mathring{\mathbf{n}} - \mathbf{D}\mathbf{n}\otimes\mathbf{n} - \mathbf{n}\otimes\mathbf{D}\mathbf{n}) - 2a(\rho)^{-1}\mathbf{D}.\end{aligned}$$

The Cauchy tensor is simplified to

$$\mathbf{T} = -\rho^2\frac{\partial\sigma}{\partial\rho}\mathbf{I} - 2\mathbb{D}(\mathbf{\Psi}^{\nabla})\mathbf{\Psi} + 2\mathbf{T}_a\mathbf{\Psi} - \rho(\nabla\mathbf{n})^T\frac{\partial\sigma}{\partial\nabla\mathbf{n}}.$$

An interesting point, deeper described in [16, 17], is the possibility to identify the coefficients of the EL theory (§2.2.2) with the parameters of the dissipation tensor (§2.3.2). Indeed the two first terms $-\rho^2\frac{\partial\sigma}{\partial\rho}\mathbf{I} - 2\mathbb{D}(\mathbf{\Psi}^{\nabla})\mathbf{\Psi}$ are equivalent to the passive dynamic of nematic liquid crystal (see the final formula for $\mathbf{T}_{EL}$ equation (2.22)), and the last terms are the same: $-\rho(\nabla\mathbf{n})^T\frac{\partial\sigma}{\partial\nabla\mathbf{n}}$.

After some computations, the following relations can be found:

$$p_{iso}(\rho) = \rho^2 \sigma_0'(\rho), \tag{2.45a}$$

$$\alpha_1 = \rho\mu\Big(\tau_2 - \frac{(a^3+1)^2}{a^3}\tau_1 + 3\tau_3\cos(\Theta)^2 + 3\tau_4\sin(\Theta)^2\Big), \tag{2.45b}$$

$$\alpha_2 = -\rho\mu(a^3-1)\tau_1, \tag{2.45c}$$

$$\alpha_3 = -\rho\mu(1-a^{-3})\tau_1, \tag{2.45d}$$

$$\alpha_4 = 2\rho\mu\tau_2, \tag{2.45e}$$

$$\alpha_5 = \rho\mu\big((1+a^3)\tau_1 - 2\tau_2\big), \tag{2.45f}$$

$$\alpha_6 = \rho\mu\big((1+a^{-3})\tau_1 - 2\tau_2\big), \tag{2.45g}$$

$$\begin{aligned}\alpha_7 =& \rho\mu\Big(\tau_2 + \tau_3\cos(\Theta)\big((3\kappa-1)\cos(\Theta) + \sqrt{2}\sin(\Theta)\big) \\ &+ \tau_4\sin(\Theta)\big((3\kappa-1)\sin(\Theta) - \sqrt{2}\cos(\Theta)\big)\Big),\end{aligned} \tag{2.45h}$$

$$\begin{aligned}\alpha_8 = \rho\mu\Big(&-\tau_2 + \frac{1}{6}\tau_3\big((9\kappa^2-6\kappa-1)\cos(2\Theta) + 9\kappa^2 \\ &+ 2\sqrt{2}(3\kappa-1)\sin(2\Theta) - 6\kappa + 3\big) - \frac{1}{6}\tau_4\big(9\kappa^2-6\kappa-1)\cos(2\Theta) - 9\kappa^2 \\ &+ 2\sqrt{2}(3\kappa-1)\sin(2\Theta) + 6\kappa - 3\big)\Big).\end{aligned} \tag{2.45i}$$

with $\kappa = \rho\frac{a'(\rho)}{a(\rho)}$.

2.4. Spontaneous flow in a two-dimensional channel

One predominant feature of active matter is its ability to generate spontaneous flow. We study a two-dimensional channel with infinite length along the x-direction and of size L along the z-direction. (see Figure2.4). The following hypotheses are taken into account:

- The material is incompressible. The pressure, becoming a Lagrangian multiplier, can be determined with one of the equations but it will be ignored during the computations. We also fix the shape parameter $a_0 = a(\rho_0)$.
- In agreement with the one constant approximation, the Oseen-Frank potential is taken as $\sigma_F = \frac{1}{2}k|\nabla\mathbf{n}|^2$.
- The infinite dimension along the x-direction allows us to assume translational invariance along x, all the unknown quantities will depend only on the transverse z variable.
- Two quantities are dealt with: the angle formed by the nematic units with the

x-axis, $\theta(z)$, and the x-component of the macroscopic velocity of the suspension, $v_x(z)$.

- No-slip boundary conditions at both extremities are assumed and $\theta(0) = \theta(L) = 0$.

In the stationary case, the equations of motion are: $\frac{\partial \mathbf{T}_{xz}}{\partial z} = 0$ and $\frac{\partial \mathbf{T}_{zz}}{\partial z} = 0$ (equation for the pressure). While the director equation becomes $\mathbf{n} \times \mathbf{h} = 0$.

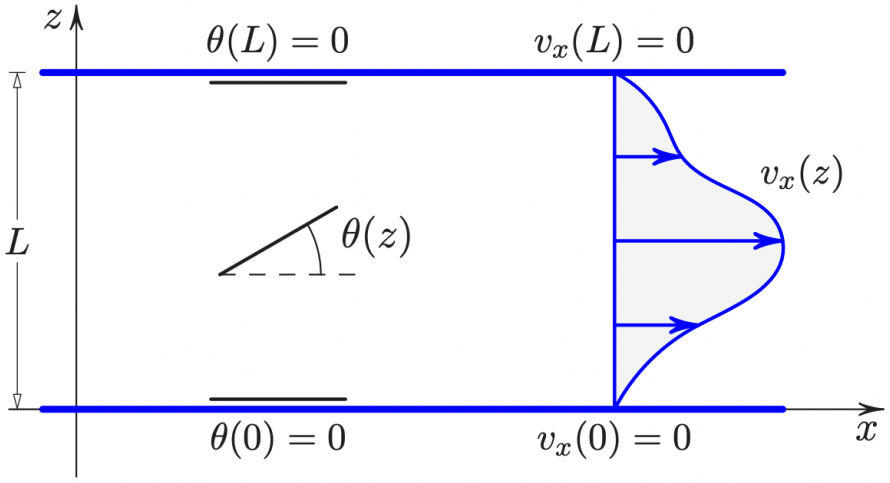

Figure 2.4: Scheme of the studied case (*source: "Active nematic gels as active relaxing solids" [17]*).

With the previous assumptions and considerations, the following equations can be obtained (see *Mathematica* code and §7.1.3),

$$4(a_0^3-1)\theta'\{2\tau v_x' \sin(2\theta)[(a_0^3-1)\cos(2\theta)+a_0^3+1]-2a_0\zeta\cos(2\theta)\}$$

$$-\tau v_x''[4(a_0^6-1)\cos(2\theta)-5a_0^6+(a_0^3-1)^2\cos(4\theta)+2a_0^3-5]=0, \tag{2.46a}$$

$$(a_0^3-1)\mu\tau v_x'[(a_0^3+1)\cos(2\theta)-a_0^3+1]+2a_0^2k\theta''=0. \tag{2.46b}$$

With the (no-slip) boundary conditions: $v_x(0) = v_x(L) = 0$ and $\theta(0) = \theta(L) = 0$. The trivial solution, $v_x(z) = 0$, $\theta(z) = 0$, is always a solution of equations (2.46a) and (2.46b). But in the next section, it will be shown that above a critical value for the activity, some non-trivial solutions appear in a neighborhood of the trivial solution.

2.4.1. Bifurcation

In order to find bifurcating solutions, equations (2.46a) and (2.46b) are linearized about the trivial solution. We find,

$$\tau v_x''(z) - \zeta a_0(a_0^3 - 1)\theta'(z) = 0, \tag{2.47a}$$

$$(a_0^3 - 1)\mu\tau v_x'(z) + a_0^2 k\theta'' = 0. \tag{2.47b}$$

When this system is solved with one boundary condition (here at $z = 0$) (see *Mathematica* code), we get

$$\theta(z) = \alpha \sin\big(\sqrt{\frac{\zeta\mu}{a_0 k}}(a_0^3 - 1)z\big) + \beta \sin^2\big(\sqrt{\frac{\zeta\mu}{a_0 k}}\frac{(a_0^3 - 1)z}{2}\big), \tag{2.48a}$$

$$v_x(z) = \frac{2a_0^2}{\tau}\sqrt{\frac{\zeta}{a_0}\frac{k}{\mu}}\big[4\alpha \sin^2\big(\sqrt{\frac{\zeta\mu}{a_0 k}}\frac{(a_0^3 - 1)z}{2}\big) - \beta \sin\big(\sqrt{\frac{\zeta\mu}{a_0 k}}(a_0^3 - 1)z\big)\big]. \tag{2.48b}$$

In general, these functions do not match the boundary condition at $z = L$ unless, $\alpha = \beta = 0$. Matching the boundary condition means to solve the equivalent algebraic problem of the form

$$A\begin{pmatrix}\alpha\\ \beta\end{pmatrix} = \begin{pmatrix}\sin\big(\sqrt{\frac{\zeta\mu}{a_0 k}}(a_0^3 - 1)L\big) & \sin^2\big(\sqrt{\frac{\zeta\mu}{a_0 k}}\frac{(a_0^3-1)L}{2}\big)\\ 4\sin^2\big(\sqrt{\frac{\zeta\mu}{a_0 k}}\frac{(a_0^3-1)L}{2}\big) & -\sin\big(\sqrt{\frac{\zeta\mu}{a_0 k}}(a_0^3 - 1)L\big)\end{pmatrix}\begin{pmatrix}\alpha\\ \beta\end{pmatrix} = 0.$$

In order to have non-trivial solutions, $\alpha \neq 0$ or $\beta \neq 0$, we need

$$\det(A) = 2\big(1 - \cos\big(\sqrt{\frac{\zeta\mu}{a_0 k}}(a_0^3 - 1)L\big)\big) = 0, \tag{2.49}$$

(see Appendix §7.1.4 for the computation) and the following critical condition between the parameters is found,

$$L\sqrt{\frac{(a_0^3 - 1)^2}{a_0}\frac{\mu\zeta}{k}} = 2\pi n,\ n \in \mathbb{N}\setminus\{0\} \Rightarrow \zeta_c = \frac{4\pi^2 a_0}{L^2(a_0^3 - 1)^2}\frac{k}{\mu}. \tag{2.50}$$

When we chose $n = 1$, ζ_c is called the critical value and is interpreted as a threshold to have the existence of non-trivial solutions. With this condition, the linearized equations

admit two independent modes of instability, indicated by the constants α (mode 1) and β (mode 2), so that we have a two-dimensional space of bifurcating solutions. This is in contrast with standard pitchfork bifurcation where there is only one mode observed. The solutions are of the form,

$$\theta(z) = \alpha \sin(\frac{2\pi n z}{L}) + \beta \sin^2(\frac{\pi n z}{L}),\ \alpha, \beta \in \mathbb{R}, \tag{2.51a}$$

$$v_x(z) = \frac{a_0(a_0^3 - 1)\zeta L}{4\pi n \tau}\left[4\alpha \sin^2(\frac{\pi n z}{L}) - \beta \sin(\frac{2\pi n z}{L})\right]. \tag{2.51b}$$

It is important to note that the amplitudes of the modes are not fixed at the linear level. We plot the two modes for each variable.

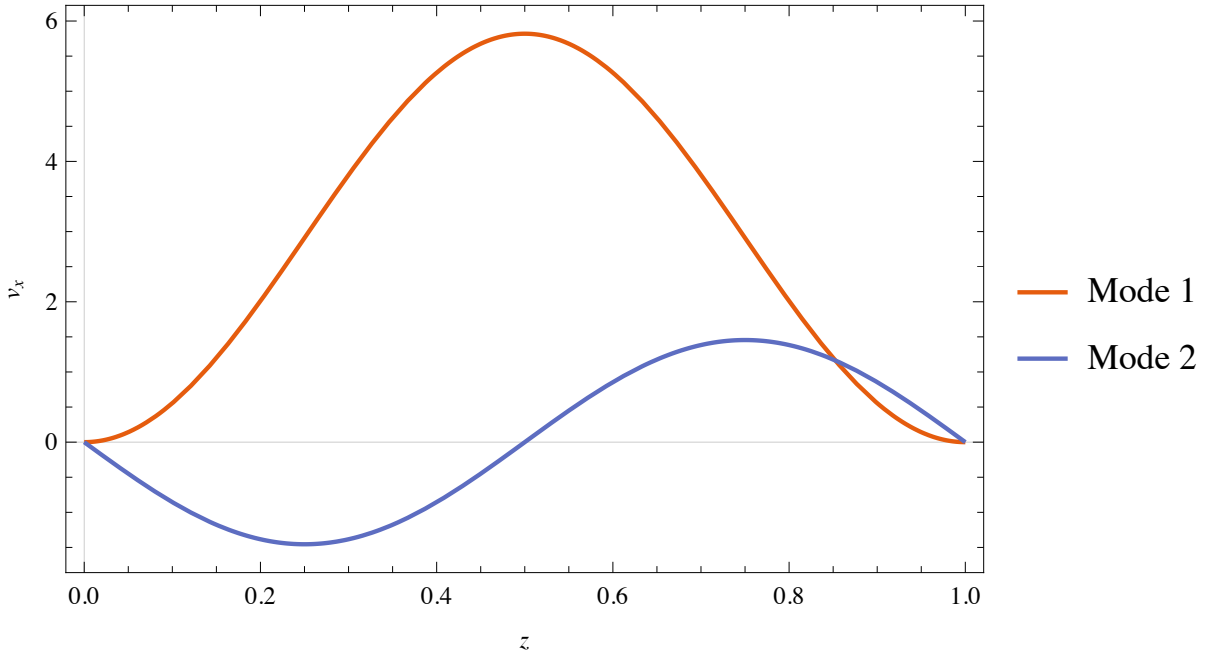

Figure 2.5: The two modes for the velocity, with values: $a_0 = 2.5$, $\tau = 1$, $\zeta_c = 0.5$, $L = 1$, $\mu = 1$. Mode 1 (α,β)=(1,0), Mode 2 (α,β)=(0,1).

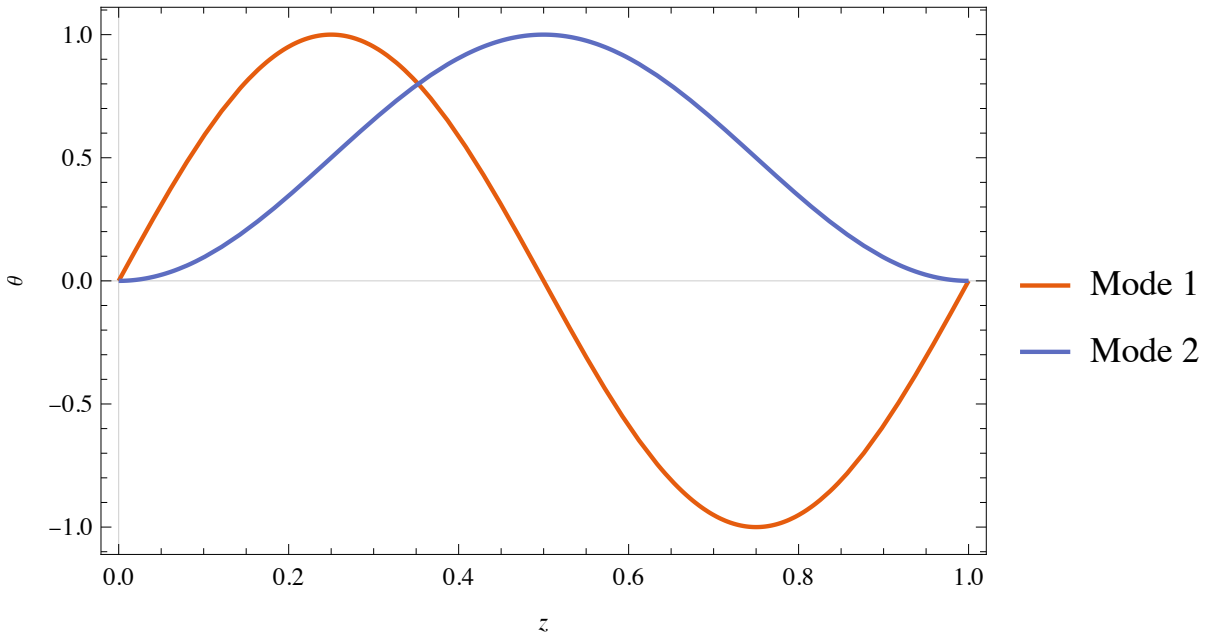

Figure 2.6: The two modes for θ, with values: $a_0 = 2.5$, $\tau = 1$, $\zeta_c = 0.5$, $L = 1$, $\mu = 1$. Mode 1 (α,β)=(1,0), Mode 2 (α,β)=(0,1).

As underlined in §2.2.3, this result is different from the classic nematic theory because we can observe at the linear level two modes instead of one. We will now test the robustness of this bifurcation to material parameter changes. We want to know if it is still possible to observe this two-fold degeneracy in three cases: the form of the active tensor $\mathbf{\Psi}$, different boundary conditions, and a change in the relaxation times.

3 | Robustness of the instability

In this chapter, we test whether the linear bifurcation analysis is robust. Indeed, some assumptions have been done to simplify the computations but other possibilities can be applied. In order to justify the work that will be exposed in the next chapter (Chapter 4) about the bifurcation, these different considerations will be tested to verify the presence of the degeneracy, and if it remains when there are material changes. The following changes will be tested:

- the active tensor will be changed,
- then different boundary conditions will be assumed,
- and finally, a second relaxation time will be taken into account in the dissipation tensor, see[16].

Then, for each one, the structure of the linear operator kernel and the critical activity are compared with the ones found in §2.4.1 and [17].
The changes in the equations will be only described for the linear ones (equations (2.47a) and (2.47b)).

3.1. Solution technique

In this section, the procedure to solve the linear equations is detailed. For every section of this chapter, a set of two equations, with two boundary conditions, form the system that has to be solved. The solving is done with *Mathematica* and using the condition at $z = 0$. For each consideration, the solution is a linear combination of two independent modes ($\mathbf{u}_1$ and $\mathbf{u}_2$).
Typically at this step, the solution is of the form $\mathbf{u} = \alpha\mathbf{u}_1 + \beta\mathbf{u}_2$, but the other boundary condition has to be applied.
They can be re-written as $\alpha\mathbf{u}_1(L) + \beta\mathbf{u}_2(L) = (0, 0)$ or algebraically

$$A \begin{pmatrix} \alpha \\ \beta \end{pmatrix} = \begin{pmatrix} 0 \\ 0 \end{pmatrix}.$$

This is a classic eigenvalue problem. To ensure the existence of non-trivial solutions, it is needed to have $\det(A) = 0$.
This will give a condition on the parameters and will allow us to define the critical parameter (in the case of a bifurcation). Three cases can be expected.

- $\det(A) \neq 0$: the kernel is reduced to the trivial solution, no bifurcation.
- $\det(A) = 0$: the kernel is one dimensional (the amplitudes α, β are related or one has to be killed). The modes are dependent or one cannot exist.
- $\det(A) = 0$: the kernel is two dimensional. The two amplitudes α, β are independent and so are the modes.

3.2. Activity tensor

In [17], the activity tensor $\mathbf{T}_a$ is said to be proportional to the identity tensor. In this section, the computations are done with the same approximations as in §2.3 but considering $\mathbf{T}_a$ proportional to the shape tensor $\mathbf{\Psi}$

$$\mathbf{T}_a = -\frac{1}{2}\mu\rho\zeta\mathbf{\Psi}. \tag{3.1}$$

This change only impacts the equation (2.46a), which becomes

$$4(a_0^3-1)\theta'\{2\tau v_x' \sin(2\theta)[(a_0^3-1)\cos(2\theta)+a_0^3+1] - 2(a_0^2+1)\zeta\cos(2\theta)\}$$

$$-\tau v_x''[4(a_0^6-1)\cos(2\theta) - 5a_0^6 + (a_0^3-1)^2\cos(4\theta) + 2a_0^3 - 5] = 0,$$

Its linearized version is

$$\tau v_x''(z) - (a_0^6-1)\zeta\theta'(z) = 0.$$

Applying the same computations (see Appendix for the solver code on *Mathematica*) the following new critical condition is found for the bifurcation

$$\sqrt{\frac{a_0^3+1}{a_0}}\sqrt{\frac{(a_0^3-1)^2\zeta\mu}{a_0 k}}L = 2\pi n.$$

The critical value is simply rescaled by a factor of $\sqrt{\frac{a_0^3+1}{a_0}}$. The structure of the kernel is identical, two independent vectors, and the modes are similar to the original case. Only the relation between the amplitudes is impacted by the rescaling. The new kernel vectors are

$$\theta(z) = \alpha \sin(\frac{2\pi n z}{L}) + \beta \sin^2(\frac{\pi n z}{L}), \tag{3.2a}$$

$$v_x(z) = \frac{(a_0^6 - 1)\zeta L}{4\pi n \tau}\left[4\alpha \sin^2(\frac{\pi n z}{L}) - \beta \sin(\frac{2\pi n z}{L})\right]. \tag{3.2b}$$

This confirms the expectations in [17], that for both cases (isotropic and non-isotropic active tensor $\mathbf{T}_a$) the results are qualitatively similar.

3.3. Boundary conditions

In [17], only homogeneous Dirichlet boundary conditions are considered, with $v_x(0) = v_x(L) = 0$. Here, the velocity is not imposed at the top of the system. We consider free boundary under atmospheric pressure. This implies no shear stress at $z = L$, i.e., $\mathbf{t} \cdot \mathbf{T}\nu = 0$.
In our case this corresponds to $\begin{pmatrix} 0 \\ 1 \end{pmatrix} \cdot \mathbf{T} \begin{pmatrix} 1 \\ 0 \end{pmatrix} = 0$. This yields on the velocity

$$v_x'(L) = 0. \tag{3.3}$$

As the equation are unchanged and only one boundary condition allows us to determine the form of the solutions, it is enough to check the existence of non-trivial solutions verifying the new boundary condition. In other words, the two modes already found (equations (2.48a) and (2.48b)) satisfy the equations and the first boundary condition (at $z = 0$) but there is a new boundary condition for the velocity at $z = L$ (see (3.3)). As explained in §3.1, we evaluate the solutions and find a condition on the parameters to have non-trivial solutions. Again, the critical value only differs by a simple rescaling,

$$2L\sqrt{\frac{(a_0^3 - 1)^2}{a_0}\frac{\mu\zeta}{k}} = 2\pi n.$$

However, the new boundary condition impacts the structure of the kernel, in fact the only possible mode is 1 (see §2.4.1). Indeed, with this new critical value, for n odd, the boundary condition for $\theta(z)$ at $z = L$ cannot be satisfied, due to the mode 2 which is

proportional to

$$\sin\left(\sqrt{\frac{\zeta\mu}{a_0 k}}\frac{(a_0^3-1)L}{2}\right)^2 = \sin\left(\frac{\pi n}{2}\right)^2 = \begin{cases} 0 \text{ if } n \text{ is even,} \\ 1 \text{ if } n \text{ is odd.} \end{cases}$$

And for all n the one of v_x is not satisfied. The spatial derivative of the velocity evaluated at $z = L$ is

$$\begin{aligned} v_x(L) =& (a_0^3-1)\frac{2a_0\zeta}{\tau}\left[2\alpha \sin\left(\sqrt{\frac{\zeta\mu}{a_0 k}}\frac{(a_0^3-1)L}{2}\right)\cos\left(\sqrt{\frac{\zeta\mu}{a_0 k}}\frac{(a_0^3-1)L}{2}\right) - \beta\cos\left(\sqrt{\frac{\zeta\mu}{a_0 k}}(a_0^3-1)L\right)\right] \\ =& -(a_0^3-1)\frac{2a_0\zeta}{\tau}\beta \implies \beta = 0. \end{aligned}$$

The kernel is only one dimensional and the vectors are of the form

$$\theta(z) = \alpha \sin(\frac{\pi n z}{L}), \tag{3.4a}$$

$$v_x(z) = \frac{2a_0(a_0^3-1)L\zeta}{n\pi\tau}\alpha \sin^2(\frac{\pi n z}{2L}). \tag{3.4b}$$

This shows that the model is sensitive to the boundary condition, indeed with the new boundary condition we break the symmetry of the system. But this point will be discussed in detail in §5.

3.4. Second relaxation time

We discussed in §2.3.2 and §2.3.3, that the remodeling of the microstructure is driven by the equation (2.35). We showed that the dissipation tensor plays a key role. The relaxation times can be related to the Leslie viscosities through the relations (2.45b)-(2.45i). However, we took a very simplified version for the dissipation tensor, assuming only one relaxation time. Now we assume that $\mathbb{D}$ has the more general form

$$\mathbb{D} = (\boldsymbol{\Psi}^{-1} \otimes \boldsymbol{\Psi}^{-1})\mathbb{T},$$

With $\mathbb{T}$ as in (2.42). In terms of Leslie coefficients, see equations (2.45b)-(2.45i), this implies considering a larger class of possible viscosity coefficients.

The equations (2.46a) and (2.46b) become

$$
\begin{aligned}
&-4\theta'\Big\{v_x'[(2(a_0^6-1)\sin(2\theta)-(1+a_0^3)^2\sin(4\theta))\tau_1\\
&+a_0^3\sin(4\theta)(\tau_2+3\cos(\Theta)\tau_d+3\tau_s)]-2a_0^2(a_0^3-1)\zeta\cos(2\theta)\Big\}\\
&-2v_x''\Big\{[1-a_0^3+(1+a_0^3)\cos(2\theta)]^2\tau_1+a_0^3\sin(2\theta)^2[\tau_s+3\cos(2\theta)\tau_d+3\tau_s]\Big\}=0,
\end{aligned}
$$

$$
(a_0^3-1)\mu\tau_1 v_x'[(a_0^3+1)\cos(2\theta)-a_0^3+1]+2a_0^3k\theta''=0.
$$

However the linearized equations are almost unaffected by the new version of the tensor, indeed only the first relaxation time enters the linear equations

$$
\begin{aligned}
\tau_1 v_x''(z)-\zeta a_0^2(a_0^3-1)\theta'(z)&=0,\\
(a_0^3-1)\mu\tau_1 v_x'(z)+a_0^3k\theta''&=0.
\end{aligned}
$$

Solving with *Mathematica* as described in §3.1, the same critical value is found

$$
L\sqrt{\frac{(a_0^3-1)^2}{a_0}\frac{\mu\zeta}{k}}=2\pi n\Rightarrow\zeta_c=\frac{4\pi^2a_0}{L^2(a_0^3-1)^2}\frac{k}{\mu}.
$$

Only the scaling of the amplitude of the two modes differs

$$
\begin{aligned}
\theta(z)=&\alpha\sin(\frac{2\pi nz}{L})+\beta\sin^2(\frac{\pi nz}{L}),\\
v_x(z)=&\frac{a_0^2(a_0^3-1)\zeta L}{4\pi n\tau_1}\big[4\alpha\sin^2(\frac{\pi nz}{L})-\beta\sin(\frac{2\pi nz}{L})\big].
\end{aligned}
$$

3.5. Summary of the results

Change in the model	equations	Critical value	Kernel dimension	Mode amplitudes
$\mathbf{T}_a \propto \mathbf{\Psi}$	changed	rescaled	2	rescaled
Boundary conditions	unchanged	rescaled	1	rescaled
$\mathbb{D} = (\mathbf{\Psi}^{-1} \otimes \mathbf{\Psi}^{-1})\mathbb{T}$	changed	unchanged	2	rescaled

To sum up, the two-fold degeneracy is robust to parameter changes. Indeed, the two modes can still be found and only a rescaling of the amplitude is noticed. Qualitatively the results are the same except for the boundary conditions. We will see that symmetry reasons are behind this degeneracy, and that the new boundary condition breaks this symmetry.

In the next chapter, we will reduce the bifurcation problem to finite dimensional and this will allows us to study the bifurcation diagram.

4 | Lyapunov-Schmidt Reduction

4.1. Lyapunov-Schmidt Reduction

The Lyapunov-Schmidt reduction is a method for simplifying the system of equations of a non-linear problem, in order to obtain the essential information about its bifurcation. In this part, the method will be briefly presented and illustrated through some examples. Then it will be applied to the equations (2.46a) and (2.46b) to study the diagram of the bifurcation presented in the previous chapters (Chapters 2 and 3).

As presented in [13], the method can be applied to any system of the form

$$\frac{dx}{dt} = F(x, \lambda). \tag{4.1}$$

A solution $x(\lambda, t)$ exhibits a bifurcation at the critical value λ_c if there is a qualitative change after this value. Considering the steady-state solutions, the equation (4.1) becomes

$$F(x, \lambda) = 0.$$

Let X, Y, and Λ (parameter space) be Banach spaces. F is a $\mathscr{C}^p$-map from the neighborhood of the critical point $(x_c, \lambda_c) \in X \times \Lambda$ to Y. We will assume that there is always a trivial solution $F(0, \lambda) = 0$, $\forall\lambda$. Assuming that $F_x(x, \lambda)$ is a Fredholm operator (see (7.2.1)), the following spaces are defined:

- $X_1 = \ker(F_x(0, \lambda))$ with finite dimension,
- $Y_1 = \text{range}(F_x(0, \lambda))$ closed subspace of Y with finite co-dimension.

Then the following spaces are considered by the direct sum over X and Y.

- $X = X_1 \oplus X_2$,
- $Y = Y_1 \oplus Y_2$, with finite dimension for Y_2.

If $\ker(F_x(0,\lambda)) = \{0\}$, then by the implicit function theorem (see §7.1) we only have a smooth solution $x = x(\lambda)$ for the equation $F(x,\lambda) = 0$ in a neighborhood of $(0,0)$. A bifurcation can only occur if $\dim(\ker(F_x(0,\lambda))) > 0$. Then, defining a projector Q onto Y_1 and writing x as $x_1 + x_2$, with $x_1 \in X_1$, $x_2 \in X_2$, the equation (4.1) is split into two new equations,

$$QF(x_1 + x_2, \lambda) = 0, \tag{4.2a}$$

$$(I - Q)F(x_1 + x_2, \lambda) = 0. \tag{4.2b}$$

For fixed λ, x_1, (4.2a) can be solved thanks to the implicit function theorem, and x_2 can be uniquely found as $x_2(x_1, \lambda)$. This form is substituted in the second equation which can be solved for x_1 and it is the bifurcation equation. It is finite-dimensional and contains all the relevant information about the nature of the bifurcation.

An interesting and important step is computing the projector Q, it will be seen that in the studied case, using the adjoint operator is useful. But before explicit the previous idea, some examples will help for a better understanding of the method.

4.2. Some basic examples

4.2.1. Example in $\mathbb{R}^2$

Let $F : \mathbb{R}^2 \times \mathbb{R} \to \mathbb{R}^2$ be,

$$F(x, y, \lambda) = (\lambda^2 + x - x^2 + y^2, \lambda + x^2 - xy).$$

It can be noticed that $(0,0,0)$ is a solution for $F(x,y,\lambda) = 0$, $\forall\lambda$. The corresponding linear operator is as follows,

$$F_{(x,y)}(x,y) = \begin{pmatrix} \frac{\partial F_1}{\partial x} & \frac{\partial F_1}{\partial y} \\ \frac{\partial F_2}{\partial x} & \frac{\partial F_2}{\partial y} \end{pmatrix} = \begin{pmatrix} 1-2x & 2y \\ 2x-y & -x \end{pmatrix} \Rightarrow F_{(x,y)}|_{(0,0)} = F_0 = \begin{pmatrix} 1 & 0 \\ 0 & 0 \end{pmatrix}.$$

One can see that the matrix cannot be inverted. Its kernel is $\mathrm{Span}\{\mathbf{e_2}\}$. Since this example is in finite dimension the range of $F_{(x,y)}|_{(0,0)}$ is found as $\mathrm{Span}\{\mathbf{e_1}\}$. We have,

$$X_1 = \mathrm{Span}\{\mathbf{e_2}\} = Y_2,$$
$$X_2 = \mathrm{Span}\{\mathbf{e_1}\} = Y_1.$$

To find Q, two methods are possible. The first one in finite dimension consists in computing the scalar product between the vectors in the base of $\mathbb{R}^2$ with the vector generating the range. The result is

$$Q = \begin{pmatrix} 0 & 0 \\ 0 & 1 \end{pmatrix}.$$

The second method that will be used in the next parts, is to find the adjoint linear operator of F_0, i.e.
Find F^* such that, for all $(x_1, y_1) \in \mathbb{R}^2$ and $(x_2, y_2) \in \mathbb{R}^2$,

$$\langle F_0(x_1, y_1), (x_2, y_2)\rangle = \langle (x_1, y_1), F^*(x_2, y_2)\rangle.$$

A little computation gives that the operator is self-adjoint, $F_0 = F^*$,

$$\langle F_0(x_1, y_1), (x_2, y_2)\rangle = \langle (x_1, 0), (x_2, y_2)\rangle = x_1 x_2 = \langle (x_1, y_1), F^*(x_2, y_2)\rangle = \langle (x_1, y_1), F_0(x_2, y_2)\rangle.$$

Having the same kernel, the projector to the adjoint kernel is obtained as in the first method:

$$P = \begin{pmatrix} 1 & 0 \\ 0 & 0 \end{pmatrix}.$$

The projector to the range of F_0 is equivalent to the identity operator minus the previous projector (see Appendix §7.2.2):

$$Q_2 = I - P = Q.$$

Then, considering that $(x, y) = \alpha \mathbf{e_1} + \beta \mathbf{e_2}$, the two-step projection is computed,

$$QF(\alpha, \beta, \lambda) = \big(0, \lambda + \alpha^2 - \alpha\beta\big) = (0, 0) \Rightarrow \beta = \frac{\lambda + \alpha^2}{\alpha}.$$

$$(I - Q)F(\alpha, \beta, \lambda) = PF(\alpha, \frac{\lambda + \alpha^2}{\alpha}, \lambda) = \lambda^2 + \alpha - \alpha^2 + \frac{\lambda^2}{\alpha^2} + 2\lambda + \alpha^2 = 0.$$

So the bifurcation equation is,

$$\alpha^3 + \lambda(2 + \lambda)\alpha^2 + \lambda^2 = 0.$$

It is possible to plot the corresponding contourline (see Figure4.1)

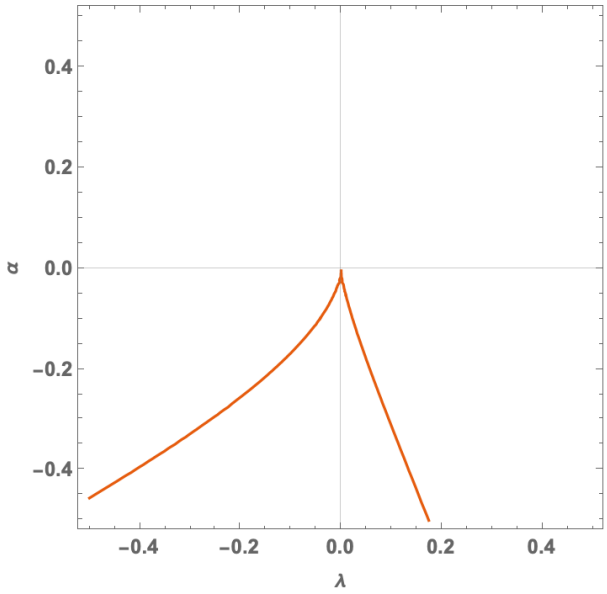

Figure 4.1: Solution of the problem by Lyapunov-Schmidt reduction (with *Mathematica*).

We observe that despite having $\ker(F_x(0,0)) \neq \{\mathbf{0}\}$ we do not have a bifurcation. This makes clear that the previous condition is only necessary but not sufficient.

4.2.2. Euler Buckling

Another interesting problem is the Euler Buckling one, which is studied in [13]. It is of a similar but simpler structure than the problem we study.

$$F(y(x), \kappa) = \frac{d^2y}{dx^2} + \kappa \sin(y) = 0.$$

x is the arc length along the deformed beam. $y(x)$ is the angle that the tangent to the beam makes with the undeformed beam and κ is the load applied to the beam in order to deform it. For $\kappa > \kappa_c$ it can be observed two possible symmetric deformations. We want to obtain the relevant information of this bifurcation by applying the Lyapunov-Schmidt reduction.

The functional $F : L^2([0,1]) \to L^2([0,1])$ is a mapping the Banach space $L^2([0,1])$ to itself. The following scalar product can be defined

$$\forall u, v \in L^2([0,1]), \quad \langle u, v \rangle = \int_0^1 u(x)v(x)dx.$$

Considering the steady solution of the problem, the equation (y' will be used for the derivative with respect to the space variable) is stated in the following way

$$\frac{d^2y}{dx^2} + \kappa \sin(y) = 0, \tag{4.3}$$

With boundary conditions

$$y'(0) = y'(1) = 0.$$

The first step is to find the kernel of the linear operator (L) corresponding to the linearized equations (4.3).

$$\mathrm{L}y = y''(x) + \kappa y(x) = 0. \tag{4.4}$$

The solution is of the form:

$$y(x) = A\cos(\sqrt{\kappa}x) + B\sin(\sqrt{\kappa}x) \Rightarrow y'(x) = \sqrt{\kappa}(-A\sin(\sqrt{\kappa}x) + B\cos(\sqrt{\kappa}x)).$$

Applying the boundary conditions, we find the following relations:

$$\begin{cases} y'(0) = B = 0, \\ y'(1) = A\sin(\sqrt{\kappa} = 0) \Rightarrow \sqrt{\kappa} = n\pi, \quad n \in \mathbb{N}. \end{cases} \Rightarrow y(x) = A\cos(n\pi x).$$

It can be observed that L is self-adjoint. In other words, the kernel of the self-adjoint operator is the same. The norm of the vector, which generates the kernel, is $\left(\int_0^1 cos(\pi x)^2\right)^{\frac{1}{2}} = \frac{1}{\sqrt{2}}$. Considering the case $n = 1$, and posing $\lambda = \kappa - \pi^2$, the solution of the non-linear equation is decomposed as in §4.1:

$$y(x) = A\cos(\pi x) + w(x, A, \lambda),$$

with the following assumptions:

- A and λ are small quantities,
- w is at least a quantity of $\mathrm{o}(A^2)$,
- w is orthogonal to the kernel of L.

The equation (4.3) is expanded to the next order to have the first non-linear terms, and

the previous form of the solution is substituted.

$$y''(x) + \kappa(y - \frac{y^3}{6}) = \frac{d^2}{dx^2}\Big(A\cos(\pi x) + w(x, A, \lambda)\Big)$$
$$+ (\lambda + \pi^2)\Big[A\cos(\pi x) + w(x, A, \lambda) - \frac{(A\cos(\pi x) + w(x, A, \lambda))^3}{6}\Big] = \mathrm{o}(A^3),$$

Finally, this simplifies to:

$$F(y, \lambda) = \lambda A\cos(\pi x) + w''(x, A, \lambda) + (\lambda + \pi^2)\Big[w(x, A, \lambda) - \frac{(A\cos(\pi x) + w(x, A, \lambda))^3}{6}\Big] = 0. \tag{4.5}$$

The equation (4.5) has to be projected to the range of L. As explained in §4.1 and in Appendix §7.2.2, F maps into a space that can be expressed as the direct sum of range(L) and its orthogonal complement ker(L*) (which is equivalent to ker(L), because the operator is self-adjoint).
Projecting into range(L) allows us to get the equation corresponding to equation (4.2a) and to find the expression of w as a function of A and λ in a unique way. In other words, the following computation is performed[1]:

$$QF(y, \lambda) = F(y, \lambda) - \langle F(y, \lambda), 2\cos(\pi x)\rangle \cos(\pi x) = 0.$$

This reads,

$$w'' + (\lambda + \pi^2)w - \frac{(\lambda + \pi^2)}{6}\Big[\frac{A^3}{4}\cos(3\pi x) + 3A^2\cos(\pi x)^2 w + 3A\cos(\pi x)w^2 + w^3\Big]$$
$$+ \cos(\pi x)\frac{\lambda + \pi^2}{6}\int_0^1 (\frac{3}{2}A^2 w\cos(3\pi x) + 3Aw^2(1 + \cos(2\pi x)) + 2w^3\cos(\pi x))dx = 0. \tag{4.6a}$$

Then, substituting the previous result in equation (4.5) and projecting it to ker(L*) allows us to obtain the bifurcation equation corresponding to equation (4.2b). This is equivalent to perform the following computation[2],

$$(I - Q)F(y, \lambda) = 0 \iff \langle F(y, \lambda), 2\cos(\pi x)\rangle = 0.$$

[1]The coefficient 2 is to have a unit-normed vector to perform the projection.
[2]Here the factor 2 is not needed but it allows us to perform the computation of the scalar product only once.

$$\lambda A - \frac{\lambda + \pi^2}{6}\left[3\frac{A^3}{4} + \int_0^1 (\frac{3}{2}A^2 w\cos(3\pi x) + 3Aw^2(1+\cos(2\pi x)) + 2w^3\cos(\pi x))dx\right] = 0. \tag{4.7}$$

With the two equations (4.6a) and (4.7) [3], some simplifications are to be considered. In equation (4.6a), taking into account the assumptions on λ and w with respect to A only the dominant terms are kept (the remaining terms are all of order $o(A^3)$) in equation (4.6a):

$$w'' + \pi^2 w - \frac{\pi^2 A^3}{24}\cos(3\pi x) = 0,$$

This is non-homogeneous ordinary differential equation:

- The homogeneous solution is $w_s(x) = B\cos(\pi x) + C\sin(\pi x)$,
- A particular solution is of the form $w_p(x) = D\cos(3\pi x) \Rightarrow w_p'(x) = -D9\pi^2\cos(3\pi x)$. So $D = -\frac{A^3}{192}$.
- The complete solution is of the form $w(x) = B\cos(\pi x) + C\sin(\pi x) - \frac{A^3}{192}\cos(3\pi x)$.
- The boundary condition $w'(0) = 0 \Rightarrow C = 0$,
- The orthogonality with the kernel requires $B = 0$.
- Finally, the solution is $w(x) = -\frac{A^3}{192}\cos(3\pi x)$.

Replacing this formula in equation (4.7) and using the same considerations between A and λ (keeping only terms bigger than $o(A^3)$), the following simplified bifurcation equation is obtained:

$$\lambda A - \frac{\pi^2 A^3}{8} = 0. \tag{4.8}$$

This allows us to observe the behavior of the solution around the bifurcation point $(0, \kappa_c = \pi^2)$. The goal of the next section is to apply this method to the problem presented in Chapter 2.

[3] See Appendix §7.2.3 for the detailed computations.

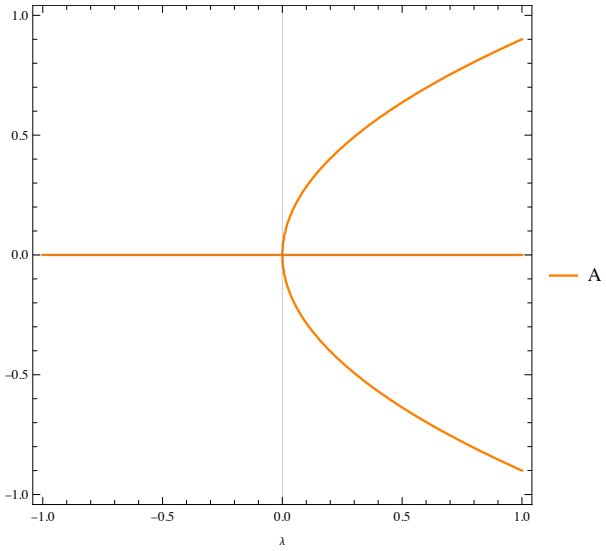

Figure 4.2: Bifurcation of the Euler buckling problem (recall: $\lambda = \kappa - \pi^2$).

We noticed that for the Euler buckling problem there is a bifurcation. For $\kappa > \pi^2 = \kappa_c$ there exist two possible non-trivial solutions in the neighborhood of the trivial solution. Their amplitude is scaled with respect to the difference between the values of the current load and the critical load.
The symmetry of the problem along the axis of the undeformed beam is also present in the nature of the bifurcation. Indeed if y is a possible solution then $-y$ is also a possible solution. The trivial solution is also still present.

4.3. Active nematic fluid

In this section, we will apply the method, previously presented, to the problem described in §2.4. The aim is to obtain more information about the two-fold degeneracy found in §2.4.1.

4.3.1. Dimensionless equations

We consider the following function space

$$\mathbb{V} = \{\mathbf{u} \in [L^2([0,1])]^2, \mathbf{u}(0) = \mathbf{u}(1) = (0,0)\}, \tag{4.9}$$

where $\mathbf{u} = (V(\xi), q(\xi))$. The scalar product is defined on V as

$$\langle \mathbf{u}, \mathbf{v} \rangle = \int_0^1 \mathbf{u} \cdot \mathbf{v} d\xi.$$

A starting point is to make equations (2.46a) and (2.46b) dimensionless. Defining L as the reference length and τ as the reference time. Then, the following dimensionless quantities are obtained:

- $\xi = \frac{z}{L}$,
- $V(\xi) = \frac{\tau}{L} v(z)$,
- $q(\xi) = \theta(z)$.
- For the derivatives, $\frac{d^n}{d\xi^n} = L^n \frac{d^n}{dz^n}$.

Another dimensionless parameter that we define, is:

$$r = \frac{\mu L^2}{k} = \left(\frac{L}{L_e}\right)^2, \tag{4.10}$$

which is the ratio of L with the "elastic length" $L_e = \sqrt{\frac{k}{\mu}}$.
The equations (2.46a) and (2.46b) become:

$$4(a_0^3 - 1)q'(\xi)\Big\{2V'(\xi)\sin(2q(\xi))\Big[(a_0^3 - 1)\cos(2q(\xi) + a_0^3 + 1)\Big] - 2a_0\zeta\cos(2q(\xi))\Big\}$$

$$-V''(\xi)\Big[4(a_0^6 - 1)\cos(2q(\xi)) - 5a_0^6 + (a_0^3 - 1)^2\cos(4q(\xi)) + 2a_0^3 - 5\Big] = 0, \tag{4.11a}$$

$$(a_0^3-1)rV'(\xi)\Big[(a_0^3+1)\cos(2q(\xi))-a_0^3+1\Big]+2a_0^2q''=0. \tag{4.11b}$$

Where the key parameters are only the anisotropic ratio a_0, r and the activity ζ. These equations are equivalent to the non-linear operator $F(V,q,\zeta)=0$ (see §4.1).

4.3.2. Linear operator and adjoint

As we did previously, we want to linearize the problem about the trivial solution (which is always a solution).We obtain the following linearized equations

$$8V''-8a_0(a_0^3-1)\zeta q'=0,$$
$$2(a_0^3-1)rV'+2a_0^2q''=0.$$

Corresponding to the linear operator L,

$$\mathrm{L}=\begin{pmatrix}8\frac{d^2}{d\xi^2} & -a\frac{d}{d\xi}\\ b\frac{d}{d\xi} & c\frac{d^2}{d\xi^2}\end{pmatrix}. \tag{4.13}$$

With: $a=8a_0(a_0^3-1)\zeta$, $b=2(a_0^3-1)r$, $c=2a_0^2$.
The adjoint operator is such as

$$\langle \mathrm{L}\begin{pmatrix}V\\q\end{pmatrix},\begin{pmatrix}U\\p\end{pmatrix}\rangle=\langle\begin{pmatrix}V\\q\end{pmatrix},\mathrm{L}^*\begin{pmatrix}U\\p\end{pmatrix}\rangle,$$

Using the boundary conditions $q(0)=q(1)=0$ and $V(0)=V(1)=0$, the double integration by parts leads to

$$\begin{aligned}\langle \mathrm{L}\begin{pmatrix}V\\q\end{pmatrix},\begin{pmatrix}U\\p\end{pmatrix}\rangle &= 8\int_0^1 V''\cdot U d\xi - a\int_0^1 q'\cdot U d\xi + b\int_0^1 V'\cdot p d\xi + c\int_0^1 q''\cdot p d\xi\\ &= 8\int_0^1 V\cdot U'' d\xi + [8V'U]_0^1 - [8VU']_0^1 + a\int_0^1 q\cdot U' d\xi - [aqU]_0^1\\ &\quad - b\int_0^1 V\cdot p' d\xi - [bpV]_0^1 + c\int_0^1 q\cdot p'' d\tilde{z} + [cpq']_0^1 - [cqp']_0^1\\ &= 8\int_0^1 V\cdot U'' d\xi - b\int_0^1 V\cdot p' d\xi + a\int_0^1 q\cdot U' d\xi + c\int_0^1 q\cdot p'' d\xi.\end{aligned}$$

So that, the adjoint operator is given by

$$\mathrm{L}^*=\begin{pmatrix}8\frac{d^2}{d\xi^2} & -b\frac{d}{d\xi}\\ a\frac{d}{d\xi} & c\frac{d^2}{d\xi^2}\end{pmatrix}. \tag{4.14}$$

Now, we look for the kernel of L^* in order to find the projectors to Y_1 and Y_2 since $\mathrm{range}(\mathrm{L}) = \ker(\mathrm{L}^*)^\perp = Y_2$ (see Appendix §7.2.2). The corresponding equations are

$$8V'' - 2(a_0^3 - 1)rq' = 0,$$

$$8a_0(a_0^3 - 1)V' + 2a_0^2 q'' = 0.$$

Solving these equations (see Appendix §7.3.3 for the *Mathematica* code), gives the following conditions on the parameters (which corresponds to the critical activity value found in §2.4.1 see equation (2.50)), we obtain a trivial kernel unless

$$\zeta_c = \frac{4a_0\pi^2}{(a_0^3 - 1)^2 r.} \tag{4.16}$$

This condition is the same for both operators, and applying the boundary conditions (same as for the solution), the kernels of both operators are found (the letter a indicates the adjoint kernel):

$$V(\xi) = \alpha(1 - \cos(2\pi\xi)) + \beta\sin(2\pi\xi),\ q(\xi) = \frac{(a_0^3 - 1)r}{2\pi a_0^2}\big(\alpha\sin(2\pi\xi) + \beta(\cos(2\pi\xi) - 1)\big),$$

$$(V(\xi), q(\xi)) = \alpha\mathbf{u}_1(\xi) + \beta\mathbf{u}_2(\xi). \tag{4.17}$$

$$\tilde{V}(\xi) = \frac{(a_0^3 - 1)r}{8\pi}\big(\alpha(\cos(2\pi\xi) - 1)\big) + \beta\sin(2\pi\xi),\ \tilde{q}(\xi) = \alpha\sin(2\pi\xi) + \beta(1 - \cos(2\pi\xi))),$$

$$(\tilde{V}(\xi), \tilde{q}(\xi)) = \alpha\mathbf{u}_{a,1}(\xi) + \beta\mathbf{u}_{a,2}(\xi). \tag{4.18}$$

It can be noticed that $\langle\mathbf{u_1}, \mathbf{u_2}\rangle = 0$ and$\langle\mathbf{u_{a,1}}, \mathbf{u_{a,2}}\rangle = 0$. The projection into the range of L (corresponding to Y_1 in§4.1) is defined as follows,

$$QF(V, q, \zeta) = F(V, q, \zeta) - \frac{1}{||\mathbf{u_{a,1}}||_{\mathbb{V}}^2}\,\langle F(V, q, \zeta), \mathbf{u_{a,1}}\rangle\ \mathbf{u_{a,1}} - \frac{1}{||\mathbf{u_{a,2}}||_{\mathbb{V}}^2}\,\langle F(V, q, \zeta), \mathbf{u_{a,2}}\rangle\ \mathbf{u_{a,2}} = 0.$$

To find the bifurcation equation $(I - Q)F(V, q, \zeta) = 0$, it is enough to impose the two scalar equations

$$\langle F(V, q, \zeta), \mathbf{u_{a,1}}\rangle = 0, \quad \langle F(V, q, \zeta), \mathbf{u_{a,2}}\rangle = 0.$$

4.3.3. Lyapunov-Schmidt reduction

We look for a solution of the form, $\Big(V(\xi), q(\xi)\Big) = \alpha \mathbf{u_1}(\xi) + \beta \mathbf{u_2}(\xi) + \Big(w_v(\xi), w_q(\xi)\Big)$.[4] With the same kind of assumptions, α and β are small quantities, the functions w_v and w_q are at least o(1) in $\alpha,\ \beta$. While in the equations the activity is expressed as $\zeta = \zeta_c(1+\lambda)$.

Because all the computations are done with *Mathematica*, the reader is invited to check the Appendix for the code and detailed equations. To make the reading easier, the expansion of the equations with respect to small quantities (here α and β) will be called $E1(\alpha, \beta, \lambda, w_v, w_q)$ for expansion of (4.11a) and $E2(\alpha, \beta, \lambda, w_v, w_q)$ for expansion of (4.11b).
A dominant balance argument on the projected equation has to be performed for eliminating higher order contributions (particularly with $\mathbf{w}$ and λ).

The first step is to solve directly the equations (4.11a) and (4.11b)with *Mathematica* in order to have the form of the wanted solution. In that way, an ansatz can be formulated,

$$\begin{cases} w_v(\xi) = \sum_{k=1}^{3} \Big(a_k(1-\cos(2k\pi\xi)) + b_k \sin(2k\pi\xi)\Big) + \xi\big(c_0 + c_1\cos(2\pi\xi) + c_2\sin(2\pi\xi)\big), \\ w_q(\xi) = \sum_{k=1}^{3} \Big(d_k(1-\cos(2k\pi\xi)) + e_k \sin(2k\pi\xi)\Big) + \xi\big(f_0 + f_1\cos(2\pi\xi) + f_2\sin(2\pi\xi)\big). \end{cases} \tag{4.19}$$

The boundary conditions and the orthogonality with respect to the kernel of L have to be respected,

$$\begin{aligned} w_v(0) = w_v(1) = 0, \\ w_q(0) = w_q(1) = 0, \\ \langle w, \mathbf{u_1}\rangle = \langle w, \mathbf{u_2}\rangle = 0. \end{aligned}$$

This allows us to impose four equations between the parameters.
Substituting the ansatz in $F(V, q, \zeta)$ the new equations are projected to the range of L (corresponding to Y_1).

$$QF(V,q,\zeta) = F(V,q,\zeta) - \frac{1}{||\mathbf{u_{a,1}}||^2_{\mathbb{V}}} \langle F(V,q,\zeta), \mathbf{u_{a,1}}\rangle\ \mathbf{u_{a,1}} - \frac{1}{||\mathbf{u_{a,2}}||^2_{\mathbb{V}}} \langle F(V,q,\zeta), \mathbf{u_{a,2}}\rangle\ \mathbf{u_{a,2}} = 0. \tag{4.20}$$

When (4.19) is inserted in (4.20) we can derive the equations among the coefficients by

[4] Let be $\mathbf{w} = \Big(w_v(\xi), w_q(\xi)\Big)$.

collecting the independent functions $\Big(\xi,\ \xi\cos(2\pi\xi),\ \xi\sin(2\pi\xi),$ $\cos(2\pi\xi),\ \cos(4\pi\xi),\ \cos(6\pi\xi),\ \sin(2\pi\xi),\ \sin(4\pi\xi),\ \sin(6\pi\xi)\Big)$. It is possible to set each coefficient to zero, thus identifying in a unique way the function $\mathbf{w}$.
Finally, this solution is substituted in $F(V,q,\zeta)$ and the bifurcation equations are derived by imposing the vanishing of the two scalar products,

$$\langle F(V,q,\zeta),\mathbf{u_{a,1}}\rangle = 0, \quad \langle F(V,q,\zeta),\mathbf{u_{a,2}}\rangle = 0. \tag{4.21}$$

Again, we keep only the leading terms of the bifurcation equations. These are

$$\alpha\Big((a_0^3-1)^2r^2(5-3a_0^3+6a_0^6)\alpha^2+(17-7a_0^3+14a_0^6)\beta^2-16a_0^4\pi^2\lambda\Big)=0, \tag{4.22a}$$

$$\beta\Big\{(a_0^3-1)^2r^2\Big((13+5a_0^3+6a_0^6)\alpha^2+(25+a_0^3+14a_0^6)\beta^2\Big)-16a_0^4\pi^2\lambda\Big\}=0. \tag{4.22b}$$

We notice that only the shape-parameter, a_0, and r influence these equations. In reality, the unique influence is from a_0 while r is just a rescaling of the amplitudes.
Indeed a direct solving of equations (4.22a) and (4.22b) gives the following possible solutions

$$\Big(\alpha=0,\ \beta=0\Big),\ \Big(\alpha=\pm\alpha(\lambda),\ \beta=0\Big),\ \Big(\alpha=0,\ \beta=\pm\beta(\lambda)\Big). \tag{4.23a}$$

$$\alpha(\lambda)=\frac{4a_0^2\pi\sqrt{\lambda}}{r\sqrt{6a_0^{12}-15a_0^9+17a_0^6-13a_0^3+5}},\ \beta(\lambda)=\frac{4a_0^2\pi\sqrt{\lambda}}{r\sqrt{14a_0^{12}-27a_0^9+37a_0^6-49a_0^3+25}} \tag{4.23b}$$

Then, the corresponding surfaces, given by (4.22a) and (4.22b), can be plotted and the intersections will give the solution.

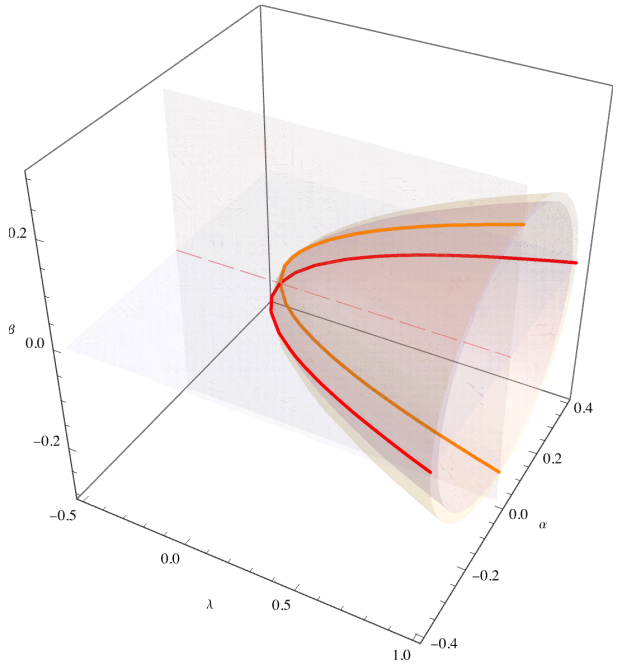

Figure 4.3: Bifurcation diagram (with *Mathematica*), as given in (4.22a) and (4.22b) with $a_0 = 2$ and $r = 1$.

Each of the two equations (4.22a), (4.22b), corresponds to two similar surfaces composed by a plane and a paraboloid. The plane corresponds to the factors α and β of each expression, in other words a zero-value can be a solution for one of the equations (4.22a) and (4.22b), the intersection of the two plans is the trivial solution.
The interesting part is the fact that the two paraboloids do not overlap (one is inside the other) and there is one intersection point at $(0, 0)$. The two intersect with the plane giving non-trivial solutions but with either $\alpha = 0$ or $\beta = 0$. No mixing of the two modes is possible, despite having $\dim(\ker(\mathrm{L})) = 2$. In Figure4.3, one can observe that the plotted lines, corresponding to the intersections of the different surfaces, all lie in one of the two planes indicating that either α or β is zero.

Thanks to this result, a simplify plot of the bifurcation can be done (see Figure 4.4). It can be clearly seen that the profiles for the amplitudes are similar. The dashed line represents the α profile, the dotted line represents the β profile and the dashed-dotted line is the trivial solution.

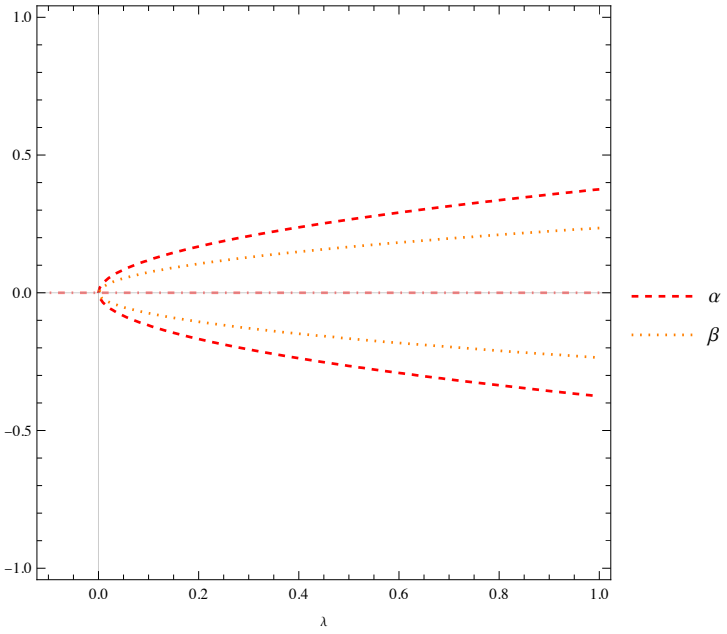

Figure 4.4: Bifurcation diagram, as given in (4.22a) and (4.22b) with $a_0 = 2$ and $r = 1$.

4.4. Numerical plots

In this section we want to check if a numerical solving of equations (4.11a) and (4.11b) is able to find the two modes for different values of activity, in other words when we move from the critical point. For that, we use the function **bvp5c** of *Matlab* which is able to solve partial differential equations with an initial guess for the solution and specific boundary conditions.

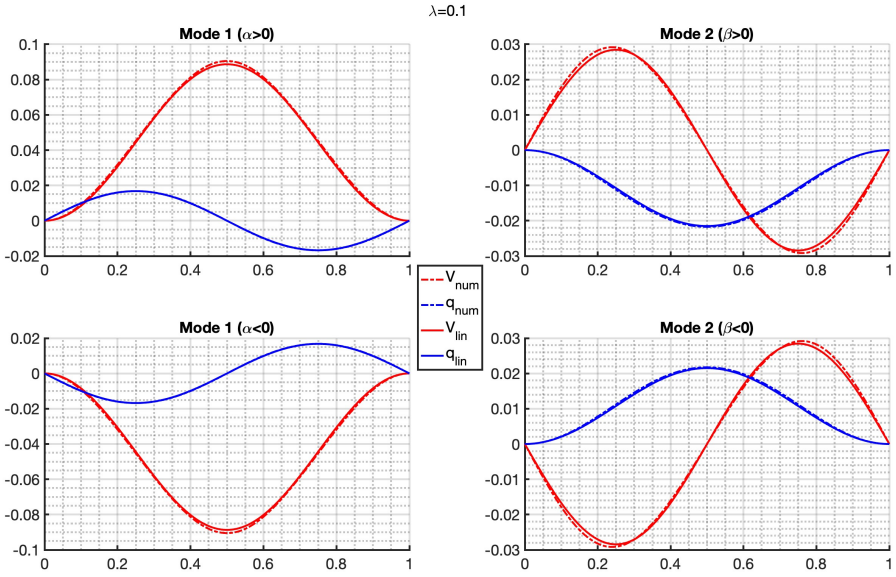

Figure 4.5: Numerical solving for $\lambda = 0.1$, forcing the modes as initial guess. Close to the critical point, the linear solutions are good approximations. V_{num} and q_{num} are the numerical solutions whereas V_{lin} and q_{lin} are the linear solutions.

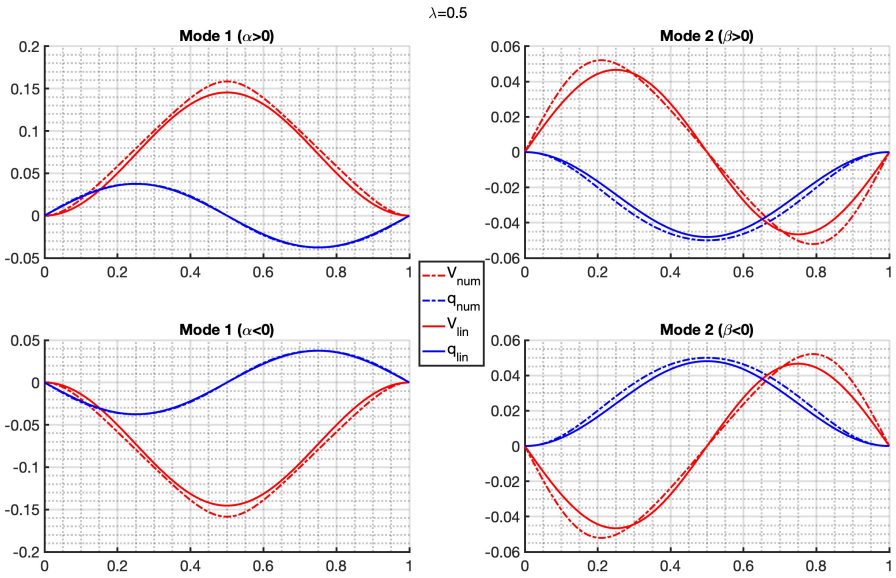

Figure 4.6: Numerical solving for $\lambda = 0.5$, forcing the modes as initial guess. Close to the critical point, the linear solutions have some problems to fit with the numerical solutions (especially mode 2).V_{num} and q_{num} are the numerical solutions whereas V_{lin} and q_{lin} are the linear solutions.

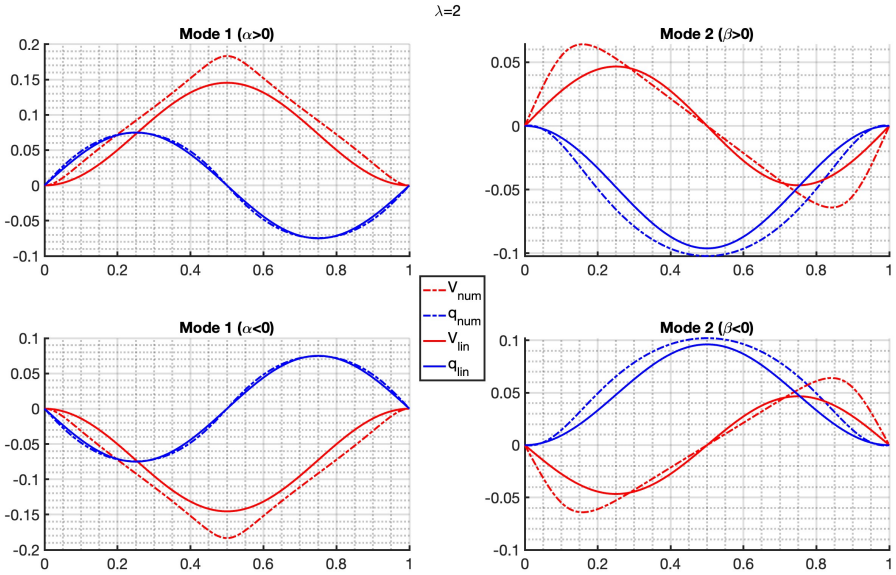

Figure 4.7: Numerical solving for $\lambda = 2$, forcing the modes as initial guess. Far from the critical point, the linear solutions are good approximations.V_{num} and q_{num} are the numerical solutions whereas V_{lin} and q_{lin} are the linear solutions.

We can see that it is possible to reach the two modes at equilibrium. However it is impossible to say if one is prefer to the other.
A possible future work could be first to draw the basin of attraction of the modes with the solving of the partial differential equations (including time). Indeed, only with a solving of the equations (4.11a) and (4.11b), when we use a higher value than the critical one, the linear modes do not fit well with the numerical solutions and it seems that the second mode is more difficult to reach with the numerical solver.
Then to study numerically the bifurcation in order to see the behavior of the different branches far from the critical point.

5 | Equivariant bifurcation analysis

In this chapter, we will show that the equations (2.46a) and (2.46b) are equivariant under the transformations of the Klein four-group. We will first present the group, then for each element we will show how it transforms the system. Finally, thanks to the generalized equivariant branching lemma, we will show that the bifurcation diagram of Figure4.3 is generic. This means that it should be observed in any model sharing the same symmetries.

5.1. Klein four-group

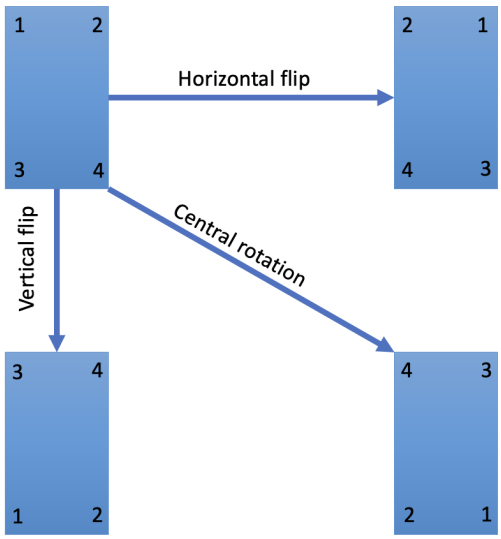

Figure 5.1: The Klein four-group as rectangle rotation: the vertical flip is $\mathbf{T}_1$, the central rotation is $\mathbf{T}_2$, and the horizontal flip is $\mathbf{T}_3$.

The Klein four-group, the simplest non-cyclic group, can be interpreted as the symmetry-group of a non-square rectangle, see Figure5.1. It contains four elements, $\mathbf{T_1}$, $\mathbf{T_2}$, $\mathbf{T_3}$ and $\mathbf{I}$ which is the identity element. As it is explained on the picture, $\mathbf{T_1}$ is the mirror reflection about the vertical axis , $\mathbf{T_2}$ is a π-rotation about the origin (or the center of the

diagonals), and $\mathbf{T_3}$ is the mirror reflection about the vertical axis. A classic representation is to consider the Klein four-group as the direct product of two cyclic groups of order two $\mathbb{Z}_2 = \{1, -1\}$, $K_4 = \mathbb{Z}_2 \times \mathbb{Z}_2$. It can be understood that in this case, there is no mixing between the axis through any deformation. That is why in $\mathbb{R}^2$,the group can be written as:

$$\mathbf{T_1} = \begin{pmatrix} 1 & 0 \\ 0 & -1 \end{pmatrix}, \quad \mathbf{T_2} = \begin{pmatrix} -1 & 0 \\ 0 & -1 \end{pmatrix}, \quad \mathbf{T_3} = \begin{pmatrix} -1 & 0 \\ 0 & 1 \end{pmatrix}, \quad \mathbf{I} = \begin{pmatrix} 1 & 0 \\ 0 & 1 \end{pmatrix}.$$

The following multiplication table shows that it is an abelian and multiplicative group[2].

$$\begin{aligned} \mathbf{T_1}^2 = \mathbf{T_2}^2 = \mathbf{T_3}^2 = \mathbf{I}, \\ \mathbf{T_1}\mathbf{T_2} = \mathbf{T_2}\mathbf{T_1} = \mathbf{T_3}, \\ \mathbf{T_1}\mathbf{T_3} = \mathbf{T_3}\mathbf{T_1} = \mathbf{T_2}, \\ \mathbf{T_2}\mathbf{T_3} = \mathbf{T_3}\mathbf{T_2} = \mathbf{T_1}. \end{aligned}$$

We will now interpret the different transformations on our problem.

5.2. Klein group and the two-dimensional channel problem

The actions of K_4 on the physical space (V,q) and on the equilibrium equations are discussed below.

- $\mathbf{T}_1$ represents a mirror symmetry of the physical system about the x-axis(see Figure 5.2).

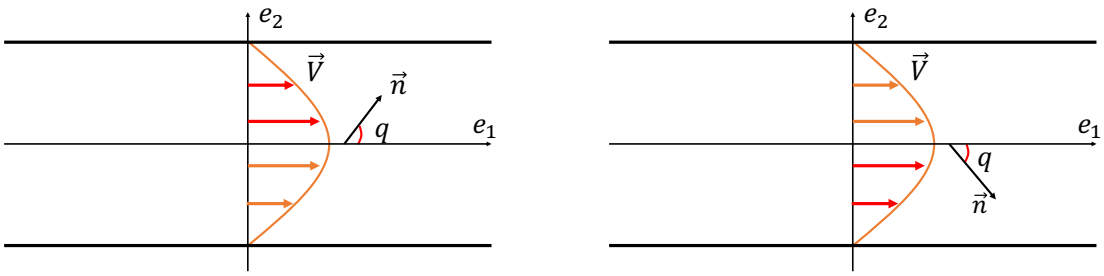

Figure 5.2: Application of the $\mathbf{e}_1$-mirror symmetry $\mathbf{T}_1$.Left picture: Initial situation, Right picture: Application of $\mathbf{T}_1$.

This is possible because the homogeneous boundary conditions do not distinguish between the top and the bottom of the channel. $\mathbf{T}_1$ corresponds to a mirror reflection of the system about the axis $\mathbf{e}_1$ as shown in Figure5.2. Hence we obtain the following transformations for the variables:

$$\begin{aligned} \xi \mapsto 1-\xi, \quad & \alpha \mapsto \alpha, \quad & \beta \mapsto -\beta, \\ \hat{V}(\xi) = & V(1-\xi), \quad & \hat{V}' = -V', \quad & \hat{V}'' = V'', \\ \hat{q}(\xi) = & -q(1-\xi), \quad & \hat{q}' = q', \quad & \hat{q}'' = -q'', \\ \sin(2\hat{q}) = & -\sin(2q), \quad & \cos(2\hat{q}) = \cos(2q), \quad & \cos(4\hat{q}) = \cos(4q). \end{aligned}$$

Substituting these relations in the equations (2.46a) and (2.46b), we observe that the first is unchanged while the second changes sign. So that $\mathbf{T}_1 F(\mathbf{u},\lambda) = F(\mathbf{T}_1\mathbf{u},\lambda)$. The same transformation holds for the vectors in the kernel of the linear operator.

By checking the bifurcation equations (4.22a) and (4.22b), we observe that the first does not change sign and the second does.

- $\mathbf{T}_2$ represents a mirror symmetry about $\mathbf{e}_2$ (see Figure 5.3) but as we will see, it is a π-rotation in the (α, β) plan.

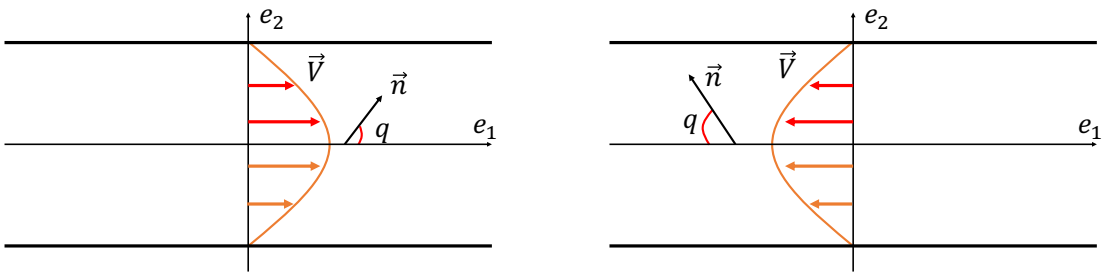

Figure 5.3: Application of the $\mathbf{e}_1$-mirror symmetry$\mathbf{T}_2$.Left picture: Initial situation, Right picture: Application of $\mathbf{T}_2$.

This symmetry is due to the infinite length of the channel, there is no condition to distinguish right and left except the choice of the notations, done by the observer. $\mathbf{T}_2$ corresponds to reversing the channel around the $\mathbf{e}_2$ axis, leading to the following transformations for the variables:

$$\begin{aligned}
\xi \mapsto & \xi, & \alpha \mapsto & -\alpha, & \beta \mapsto & -\beta, \\
\hat{V}(\xi) = & -V(\xi), & \hat{V}' = & -V', & \hat{V}'' = & -V'', \\
\hat{q}(\xi) = & \pi - q(\xi), & \hat{q}' = & -q', & \hat{q}'' = & -q'', \\
\sin(2\hat{q}) = & -\sin(2q), & \cos(2\hat{q}) = & \cos(2q), & \cos(4\hat{q}) = & \cos(4q).
\end{aligned}$$

Substituting these relations in the equations (2.46a) and (2.46b), we remark that this time both equations change sign. We applied $\mathbf{T}_2$ to the equations. The same transformation holds for the vectors in the kernel of the linear operator.
Both equations (4.22a) and (4.22b) change sign.

- Nematic symmetry is automatically satisfied by our equations and behaves as the identity element of K_4. (see Figure 5.4):

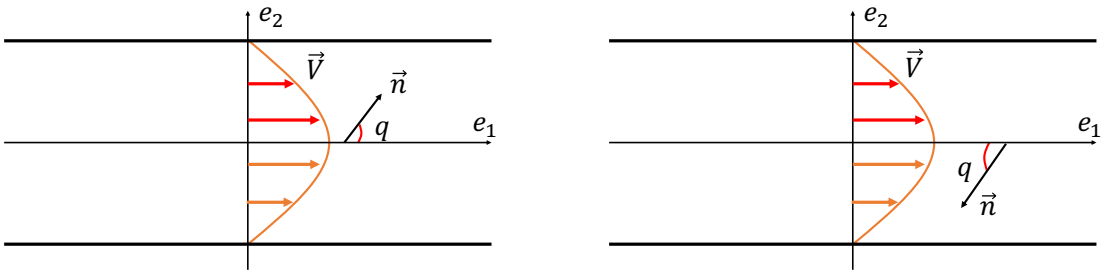

Figure 5.4: The nematic symmetry (**I**). Left picture: Initial situation, Right picture: Nematic symmetry.

The nematic symmetry is very particular. It means that the the quantities are invariant with respect to the orientation of the director. This corresponds to the following changes:

$$\begin{aligned}
\hat{\mathbf{n}} &\mapsto -\mathbf{n} & \xi &\mapsto \xi, & \alpha &\mapsto \alpha, & \beta &\mapsto \beta,\\
\hat{V}(\xi) &= V(\xi), & \hat{V}' &= V', & \hat{V}'' &= V'',\\
\hat{q}(\xi) &= \pi + q(\xi), & \hat{q}' &= q', & \hat{q}'' &= q'',\\
\sin(2\hat{q}) &= \sin(2q), & \cos(2\hat{q}) &= \cos(2q), & \cos(4\hat{q}) &= \cos(4q).
\end{aligned}$$

Substituting these relations in the equations (2.46a) and (2.46b), we remark that both equations do not change sign. We applied **I** to the equations. The transformation holds for the vectors in the kernel of the linear operator.
For the equations (4.22a) and (4.22b), both are unchanged. The nematic symmetry coincides with the identity **I**.

- $\mathbf{T}_3$ is the composition of $\mathbf{T}_1$ and $\mathbf{T}_2$ (see Figure 5.5). In physical terms it corresponds to a π-rotation about $\mathbf{e}_3$ of the system.

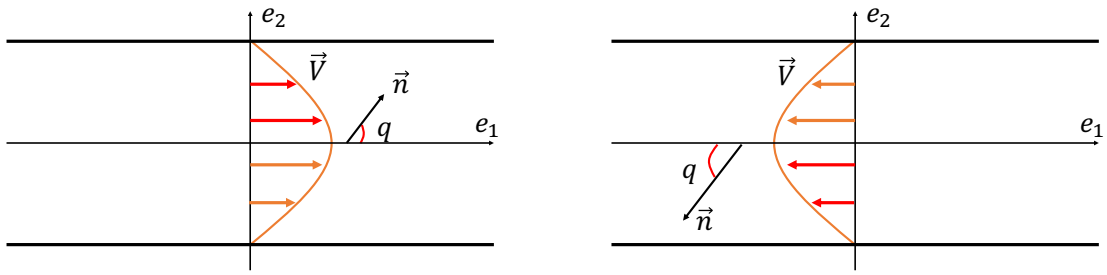

Figure 5.5: Composition of $\mathbf{T}_1$ and $\mathbf{T}_2$: the transformation $\mathbf{T}_3$.Left picture: Initial situation, Right picture: Application of $\mathbf{T}_3$.

It can be interpreted as the following transformation for the variables:

$$\begin{aligned} \xi \mapsto & 1-\xi, & \alpha \mapsto & -\alpha, & \beta \mapsto & \beta, \\ \hat{V}(\xi) = & -V(1-\xi), & \hat{V}' = & V', & \hat{V}'' = & -V'', \\ \hat{q}(\xi) = & \pi + q(1-\xi), & \hat{q}' = & -q', & \hat{q}'' = & q'', \\ \sin(2\hat{q}) = & \sin(2q), & \cos(2\hat{q}) = & \cos(2q), & \cos(4\hat{q}) = & \cos(4q). \end{aligned}$$

Substituting these relations in the equations (2.46a) and (2.46b), we observe that the first equation changes sign while the other is unchanged. So again $\mathbf{T}_3 F(\mathbf{u}, \lambda) = F(\mathbf{T}_3\mathbf{u}, \lambda)$. The same transformation holds for the vectors in the kernel of the linear operator.
For the equations (4.22a) and (4.22b), the first changes sign and the second is unchanged.

Therefore, equations (2.46a)-(2.46b), and (4.22a)-(4.22b) are K_4-equivariant. This means that

$$\mathbf{T}_k F(\lambda, \mathbf{x}) = F(\lambda, \mathbf{T}_k\mathbf{x}), \quad \forall \lambda,\ \mathbf{x},\ \mathbf{T}_k \tag{5.1}$$

Now, we will state some theory in order to interpret the previous observations as bifurcation results.

5.3. Fixed-point subspace and the Generalized equivariant branching lemma

In this section, we will use the equivariant branching lemma to draw conclusions about the generic bifurcation in our system, as described in [7]. The K_4 has two trivial subgroups ($\Sigma_0 = \{\mathbf{I}\}$, and $\Sigma_4 = K_4$) and three proper subgroups ($\Sigma_1 = \{\mathbf{I}, \mathbf{T}_1\}$, $\Sigma_2 = \{\mathbf{I}, \mathbf{T}_2\}$, and $\Sigma_3 = \{\mathbf{I}, \mathbf{T}_3\}$). For any subgroup Σ, we define the fixed-point subspace as follows (we call $\mathbb{V}$ the vector space where the transformations are applied),

$$\mathrm{Fix}(\Sigma) = \{\mathbf{x} \in \mathbb{V},\ \mathbf{T}_j\mathbf{x} = \mathbf{x},\ \forall\ \mathbf{T}_j \in \Sigma\}.$$

Every fixed-point subspace is non-empty because it contains at least $\{\mathbf{0}\}$, and closed, by the linearity of the transformation every linear combination of two fixed-points is still a fixed-point. In addition, the fixed-point subspace are flow-invariant, i.e., the flow of the dynamical system remains in $\mathrm{Fix}(\Sigma)$ if starts in $\mathrm{Fix}(\Sigma)$. Indeed, posing $\mathbf{U} = (V, q)$ taking the operator F corresponding to our problem, we have,

$$\forall\ \mathbf{T}_i \in \Sigma,\ \mathbf{T}_i F(\mathbf{U}, \zeta) = F(\mathbf{T}_i\mathbf{U}, \zeta) = F(\mathbf{U}, \zeta),\ \forall\ \mathbf{U} \in \mathrm{Fix}(\Sigma).$$

Therefore $F(\mathrm{Fix}(\Sigma), \zeta) \subset \mathrm{Fix}(\Sigma)$, so that $F(\cdot, \zeta)$ maps $\mathrm{Fix}(\Sigma)$ to $\mathrm{Fix}(\Sigma)$ and the bifurcation analysis can be restricted $\mathrm{Fix}(\Sigma)$. A related concept is that of stabilizer subgroup. Given $\mathbf{x} \in V$, the stabilizer of $\mathbf{x}$ is defined as

$$\mathrm{Stab}(\mathbf{x}) = \big\{\mathbf{T}_g \in K_4,\ \mathbf{T}_g\mathbf{x} = \mathbf{x}\big\}.$$

Now, we find the fixed points and the stabilizers in our problem, considering the plan (α, β).

- $(\alpha, \beta) = (1, 0)$ is fixed by Σ_1. So $\mathrm{Stab}\big((1,0)\big) = \Sigma_1$ and $\mathrm{Fix}(\Sigma_1) = \mathrm{Span}\big\{\mathbf{e}_1\big\} \cong \mathbb{R}$.
- $(\alpha, \beta) = (0, 1)$ is fixed by Σ_3. So $\mathrm{Stab}\big((0,1)\big) = \Sigma_3$ and $\mathrm{Fix}(\Sigma_3) = \mathrm{Span}\big\{\mathbf{e}_2\big\} \cong \mathbb{R}$.
- No point, other than the origin, is fixed by Σ_2. So $\mathrm{Fix}(\Sigma_2) = \big\{\mathbf{0}\big\}$.
- All points are fixed by $\{\mathbf{I}\}$. So $\mathrm{Fix}(\{\mathbf{I}\}) = \mathrm{Span}\big\{\mathbf{e}_1, \mathbf{e_2}\big\} \cong \mathbb{R}^2$.

As we showed in the previous section §5.2, we have the following results:

Stabilizers subgroups	dim(Fix(Σ))	non trivial changes in $(\alpha,\ \beta)$	$\ker(L) \cap \mathrm{Fix}(\Sigma)$
K_4	0	/	$\{\mathbf{0}\}$
$\{\mathbf{I}\}$	2	no change	$\mathrm{Span}\{\mathbf{u}_1, \mathbf{u}_2\}$
Σ_1	1	$\alpha \mapsto \alpha,\ \beta \mapsto -\beta$	$\mathrm{Span}\{\mathbf{u}_1\}$
Σ_2	0	$\alpha \mapsto -\alpha,\ \beta \mapsto -\beta$	$\{\mathbf{0}\}$
Σ_3	1	$\alpha \mapsto -\alpha,\ \beta \mapsto \beta$	$\mathrm{Span}\{\mathbf{u}_2\}$

Now, we state the main theorem which will allow us to understand the bifurcation diagram through the symmetries.

Theorem 5.1 (Generalized equivariant branching lemma)**.** *Let* Γ *be a finite group or a compact Lie group acting on a real vector space,* $\mathbb{V}$*, with* $\mathrm{Fix}(\Gamma) = \{\mathbf{0}\}$*.*
Let

$$F(\mathbf{U}, \lambda) = 0, \tag{5.2}$$

be a Γ*-equivariant bifurcation problem with* $DF|_{(\mathbf{0},\lambda_c)}\mathbf{W} = 0$ *and* $DF_\lambda|_{(\mathbf{0},\lambda_c)}\mathbf{W} \neq 0$ *for nonzero* $\mathbf{W} \in \mathrm{Fix}(\Sigma)$*, where* Σ *is a stabilizer subgroup of* Γ*. Then, if* Σ *satisfies:*

$$\dim(\mathrm{Fix}(\Sigma)) = 1, \tag{5.3}$$

there is a smooth solution branch $\mathbf{U} = s\mathbf{W},\ \lambda = \lambda(s)$ *to* $F(\mathbf{U}, \lambda) = 0$*.*

In our case, $\Gamma = K_4$, $\mathbf{W}$ is either $\mathbf{u}_1$ or $\mathbf{u}_2$ as defined in equations (4.17).

Applying the theorem 5.1, we understand that the only possible branches share the symmetry of either Σ_1 or Σ_3 which correspond respectively to the mode 1 and 2, defined in equations (2.51a) and (2.51b). This result confirms that the branches do not mix, except for the trivial solution. Furthermore, for any generic system possessing K_4 symmetry should show the same bifurcation diagram, with two separate branches of pitchfork type.

6 | Conclusion

In this thesis, we analyzed the spontaneous flow arising in an alternative model for active matter. Classic theories, based on the Eriksen-Leslie theory, extend the passive theory by adding an active stress in a way that is not universally accepted due to some incoherence with the irreversible thermodynamics. The alternative model, studied here, is able to avoid the previous incoherences. A characteristic behavior of active nematics, the spontaneous flow, arises with two modes of instability. By contrast classic theories based on liquid crystals only show one mode.
We showed that the instability is robust to parameter changes and seems to be a general feature of the model. Yet, we noticed that breaking the symmetries through boundary condition change, we loose the two-fold degeneracy.

By performing the Lyapunov-Schmidt reduction, we were able to transform the bifurcation problem into a finite-dimensional one and we drew the bifurcation diagram. This allowed us to see that the two modes exist for any dimensionless parameters. The solutions are only rescaled by a parameter change. In addition, the modes at equilibrium do not mix and there is no evidence that one is prefer over the other.
Finally, we showed how these results can be explained looking at the symmetries: the system and its equations are K_4-equivariant. Explicitly, the symmetries are the nematic symmetry (molecules have head-tail symmetry), mirror symmetry with respect to the $\mathbf{e}_z$-axis due to the infinite length of the channel along $\mathbf{e}_x$, and mirror symmetry about the $\mathbf{e}_x$-axis provided that also the boundary conditions are symmetric. The generalized equivariant branching lemma confirms the results of the bifurcation and their generality to every system possessing the same symmetries.

To better understand the behavior of the bifurcation, future works could deal with the study of numerical problem. The idea would be to build numerically the basin of attraction of each mode and get a complete diagram of the bifurcation, also in a dynamical regime.

With these tools completed the comparison with similar results in classic theory [10, 19] could be explicitly done.

7 | Appendix

7.1. Appendix Chapter 2

7.1.1. Comparison: EL rate of dissipation and energy loss in (AM) model

Let recall the two formula, for EL theory

$$\int_V \rho(\mathbf{f}\cdot\mathbf{v}+\mathbf{K}\cdot\mathbf{w})\,dV+\int_S(\mathbf{t}\cdot\mathbf{v}+\mathbf{l}\cdot\mathbf{w})\,dS=\frac{D}{Dt}\int_V(\frac{1}{2}\rho\mathbf{v}\cdot\mathbf{v}+w_F)\,dV+\int_V\mathscr{D}_{EL}\,dV.$$

for the alternative active model,

$$\mathscr{D}:=W^{ext}-\dot{K}-\dot{\mathscr{F}}\geq 0,$$

with

$$W^{ext}:=\int_{\mathscr{P}_t}\mathbf{b}\cdot\mathbf{v}dv\;+\int_{\partial\mathscr{P}_t}\mathbf{t}_\nu\cdot\mathbf{v}da\;+\int_{\mathscr{P}_t}\mathbf{g}\cdot\dot{\mathbf{n}}dv\;+\int_{\partial\mathscr{P}_t}\mathbf{m}_\nu\cdot\mathbf{n}da\;+\int_{\mathscr{P}_t}\mathbf{T}_a\cdot\mathbf{B}_e^{\nabla}dv,$$
$$K+\mathscr{F}:=\int_{\mathscr{P}_t}\Big(\frac{1}{2}\rho\mathbf{v}^2+\rho\sigma(\rho,\mathbf{B}_e,\mathbf{n},\nabla\mathbf{n})\Big)dv.$$

we can easily identify the following:

- $\rho\mathbf{f}=\mathbf{b}$ for the external force body.
- The most evident $\mathbf{t}=\mathbf{t}_\nu$ external traction on the surface.
- $\mathbf{n}\times\mathbf{g}=\rho\mathbf{K}$ for the external body moment. Indeed, $\mathbf{g}\cdot\dot{\mathbf{n}}=\mathbf{g}\cdot(\mathbf{w}\times\mathbf{n})=(\mathbf{g}\times\mathbf{n})\cdot\mathbf{w}=\rho\mathbf{K}\cdot\mathbf{w}$.
- Same manipulation to get $\mathbf{n}\times\mathbf{m}_\nu=\mathbf{l}$, the surface body moment per unit area.
- K can be easily identify and $\mathscr{F}$ was identified when introducing the Oseen-Frank potential.

- Finally, if the term depending on activity vanishes we can identify $\mathscr{D} = \int_V \mathscr{D}_{EL}\, dV$.

7.1.2. Computation of $\frac{\partial \sigma}{\partial \mathbf{B}_e}$

To make the dissipation inequality (2.26) explicit, we need to compute the quantity $\frac{\partial \sigma}{\partial \mathbf{B}_e}$. We recall that the free-energy density is

$$\sigma(\rho, \mathbf{B}_e, \mathbf{n}, \nabla \mathbf{n}) = \sigma_0(\rho) + \frac{1}{2}\mu\Big(\mathrm{tr}(\mathbf{\Psi}^{-1}\mathbf{B}_e) - \log(\det(\mathbf{\Psi}^{-1}\mathbf{B}_e))\Big) + \sigma_F(\rho, \mathbf{n}, \nabla \mathbf{n}).$$

To compute the derivative with respect to $\mathbf{B}_e$, we introduce the small quantity $\epsilon\mathbf{B}$ which is a symmetric tensor. Then using the fact that $\det(\mathbf{\Psi}) = 1$, we get

$$\begin{aligned}\sigma(\rho, \mathbf{B}_e + \epsilon\mathbf{B}, \mathbf{n}, \nabla \mathbf{n}) - \sigma(\rho, \mathbf{B}_e, \mathbf{n}, \nabla \mathbf{n}) =& \frac{\mu}{2}\Big(\mathbf{\Psi}^{-1}\epsilon\mathbf{B} \cdot \mathbf{I} - \log(\det(\mathbf{I} + \epsilon\mathbf{B}\mathbf{B}_e^{-1}))\Big) \\ =& \frac{\mu}{2}\Big(\mathbf{\Psi}^{-1} \cdot \epsilon\mathbf{B} - \log(\det(\mathbf{I} + \epsilon\mathbf{B}\mathbf{B}_e^{-1}))\Big).\end{aligned}$$

We use the two following approximations

$$\det(\mathbf{I} + \epsilon\mathbf{B}\mathbf{B}_e^{-1}) \approx 1 + \epsilon\mathbf{B}\mathbf{B}_e^{-1} \cdot \mathbf{I} + \mathrm{o}(\epsilon),$$

$$\log(1 + \epsilon\mathbf{B}\mathbf{B}_e^{-1} \cdot \mathbf{I}) \approx \epsilon\mathbf{B}\mathbf{B}_e^{-1} \cdot \mathbf{I} = \mathbf{B}_e^{-1} \cdot \epsilon\mathbf{B} + \mathrm{o}(\epsilon).$$

Substituting this result in the previous computation, and dividing by ϵ, we get

$$\frac{\partial \sigma}{\partial \mathbf{B}_e} = \frac{\mu}{2}\big(\mathbf{\Psi}^{-1} - \mathbf{B}_e^{-1}\big).$$

7.1.3. Derivations of equations (2.46a) and (2.46b)

In this part, for simplicity we use in some computation the Einstein notation,

$$\sum_j u_j v_j = u_j v_j.$$

With the simplifications, the Cauchy tensor becomes,

$$\mathbf{T} = -\rho^2 \frac{\partial \sigma}{\partial \rho}\mathbf{I} - \rho\mu\big(\tau \mathbf{\Psi}^{\nabla}\mathbf{\Psi} + \zeta\mathbf{\Psi}\big) - \rho\big(\nabla \mathbf{n}\big)^T \frac{\partial \sigma}{\partial \nabla \mathbf{n}}.$$

The gradient of the director is obtained as follows,

$$\nabla \mathbf{n} = \theta'(z)[\cos(\theta(z))\mathbf{e}_z - \sin(\theta(z))\mathbf{e}_x] \otimes \mathbf{e}_z = \theta'(z)\mathbf{n}^{\perp} \otimes \mathbf{e}_z.$$

The only part depending on it in the free-energy density is the Frank-Oseen potential, thereby,

$$-\rho\big(\nabla\mathbf{n}\big)^T\frac{\partial\sigma}{\partial\nabla\mathbf{n}}=-\rho\big(\nabla\mathbf{n}\big)^T\frac{\partial}{\partial\nabla\mathbf{n}}\Big(\frac{1}{2}k|\nabla\mathbf{n}|^2\Big)=-\rho k\big(\nabla\mathbf{n}\big)^T\big(\nabla\mathbf{n}\big)=-\rho k\theta'(z)^2\mathbf{e}_z\otimes\mathbf{e}_z.$$

Now, focusing on the codeformational derivative $\mathbf{\Psi}^{\nabla}$, we recall that $\mathbf{\Psi}=a_0^2(\mathbf{n}\otimes\mathbf{n})+a_0^{-1}(\mathbf{I}-\mathbf{n}\otimes\mathbf{n})$, we can notice that $\frac{\partial\mathbf{\Psi}}{\partial t}=0$. Then according to the following formula for the gradient of tensor in Cartesian coordinates,

$$\nabla\mathbf{\Psi}=\frac{\partial\mathbf{\Psi}_{ij}}{\partial x_k}\mathbf{e}_i\otimes\mathbf{e}_j\otimes\mathbf{e}_k=\frac{\partial\mathbf{\Psi}_{ij}}{\partial z}\mathbf{e}_i\otimes\mathbf{e}_j\otimes\mathbf{e}_z.$$

As the velocity is $\mathbf{v}=v_x(z)\mathbf{e}_x$, we have directly $\nabla\mathbf{\Psi}\mathbf{v}=0$.

The computation of the codeformational derivative is restrained to

$$\begin{aligned}\mathbf{\Psi}^{\nabla}=&\frac{\partial\mathbf{\Psi}}{\partial t}+(\nabla\mathbf{\Psi})\mathbf{v}-(\nabla\mathbf{v})\mathbf{\Psi}-\mathbf{\Psi}(\nabla\mathbf{v})^T\\=&-(\nabla\mathbf{v})\mathbf{\Psi}-\mathbf{\Psi}(\nabla\mathbf{v})^T\\=&-(a_0^2-a_0^{-1})v_x'(x)\sin(\theta(z))(\mathbf{e}_x\otimes\mathbf{n}+\mathbf{n}\otimes\mathbf{e}_x)-a_0^{-1}(\mathbf{e}_x\otimes\mathbf{e}_z+\mathbf{e}_z\otimes\mathbf{e}_x).\end{aligned}$$

The Stokes equations are retrained to

$$\frac{\partial\mathbf{T}_{xz}}{\partial z}=0,\quad\frac{\partial\mathbf{T}_{zz}}{\partial z}=0.$$

The first will give us the pressure equation and the second after some computations is equivalent to

$$\begin{aligned}-\frac{\rho\mu}{8a_0^2}\frac{d}{dz}\Big(&4a_0(a_0^3-1)\zeta\sin(2\theta(z))+\tau v_x'(z)[4(a_0^6-1)\cos(2\theta(z))\\&-5a_0^6+(a_0^3-1)^2\cos(4\theta(z))+2a_0^3-5]\Big)=0.\end{aligned}$$

We get equation(2.46a).

For the equation (2.46b), we first need to compute the molecular field

$$\mathbf{h}:=\rho\frac{\partial\sigma}{\partial\mathbf{n}}-\mathrm{div}\Big(\rho\frac{\partial\sigma}{\partial\nabla\mathbf{n}}\Big).$$

We observe that

$$\frac{\partial\sigma}{\partial\mathbf{n}}=\frac{\partial\sigma}{\partial\mathbf{\Psi}}\frac{\partial\mathbf{\Psi}}{\partial\mathbf{n}}=2(a_0^2-a_0^{-1})\frac{\partial\sigma}{\partial\mathbf{\Psi}}\mathbf{n},$$

Then, considering the unit determinant property of the shape tensor, we have the following

expression for the free-energy density

$$\sigma(\rho, \mathbf{B}_e, \mathbf{n}, \nabla\mathbf{n}) = \sigma_0(\rho) + \frac{1}{2}\mu\Big(\mathrm{tr}(\boldsymbol{\Psi}^{-1}\mathbf{B}_e) - \log(\det(\mathbf{B}_e))\Big) + \sigma_F(\rho, \mathbf{n}, \nabla\mathbf{n}).$$

We derive the previous expression with respect to the shape tensor $\boldsymbol{\Psi}$, the computation is reduced to

$$\frac{\partial\sigma}{\partial\boldsymbol{\Psi}} = \frac{\partial}{\partial\boldsymbol{\Psi}}\Big(\frac{1}{2}\mu\ \mathrm{tr}(\boldsymbol{\Psi}^{-1}\mathbf{B}_e)\Big).$$

Considering $\boldsymbol{\Psi}_1$ having the same properties as the shape tensor $\boldsymbol{\Psi}$ and ϵ a small quantity, we compute the derivative as follows

$$\begin{aligned}\big(\boldsymbol{\Psi} + \epsilon\boldsymbol{\Psi}_1\big)^{-1}\mathbf{B}_e\cdot\mathbf{I} - \boldsymbol{\Psi}^{-1}\mathbf{B}_e\cdot\mathbf{I} =& \boldsymbol{\Psi}^{-1}\big(\mathbf{I} + \epsilon\boldsymbol{\Psi}_1\boldsymbol{\Psi}^{-1}\big)^{-1}\mathbf{B}_e\cdot\mathbf{I} - \boldsymbol{\Psi}^{-1}\mathbf{B}_e\cdot\mathbf{I}\\ \simeq& \boldsymbol{\Psi}^{-1}\big(\mathbf{I} - \epsilon\boldsymbol{\Psi}_1\boldsymbol{\Psi}^{-1}\big)\mathbf{B}_e\cdot\mathbf{I} - \boldsymbol{\Psi}^{-1}\mathbf{B}_e\cdot\mathbf{I}\\ =& -\boldsymbol{\Psi}^{-2}\mathbf{B}_e\cdot\epsilon\boldsymbol{\Psi}_1 = -\boldsymbol{\Psi}^{-1}\mathbf{B}_e\boldsymbol{\Psi}^{-1}\cdot\epsilon\boldsymbol{\Psi}_1.\end{aligned}$$

We can compute $\boldsymbol{\Psi}\mathbf{n} = a_0^2\mathbf{n}$, and $\boldsymbol{\Psi}^{-1}\mathbf{n} = a_0^{-2}\mathbf{n}$, leading to

$$\frac{\partial\sigma}{\partial\mathbf{n}} = -\mu(1 - a_0^{-3})\boldsymbol{\Psi}^{-1}\mathbf{B}_e\mathbf{n}.$$

We need to compute

$$\begin{aligned}\mathrm{div}\Big(\frac{\partial\sigma}{\partial\nabla\mathbf{n}}\Big) =& k\mathrm{div}(\nabla\mathbf{n}),\\ \mathrm{div}(\mathbf{T}) =& \frac{\partial\mathbf{T}_{ij}}{\partial x_j}\mathbf{e}_i,\\ k\mathrm{div}(\nabla\mathbf{n}) =& k\frac{\partial(\nabla\mathbf{n})_{ij}}{\partial x_j}\mathbf{e}_i = k(\theta''(z)\mathbf{n}^\perp - \theta'(z)^2\mathbf{n}).\end{aligned}$$

Finally,

$$\mathbf{h} = -\rho\mu(1 - a_0^{-3})\boldsymbol{\Psi}^{-1}\mathbf{B}_e\mathbf{n} - k(\theta''(z)\mathbf{n}^\perp - \theta'(z)^2\mathbf{n}.$$

In the previous section §7.1.2, we expressed $\frac{\partial\sigma}{\partial\mathbf{B}_e}$ in two ways. That allows us to write the following relation

$$\begin{aligned}\frac{\rho\mu}{2}(\boldsymbol{\Psi}^{-1}\mathbf{B}_e - \mathbf{I}) =& \mathbf{T}_a\mathbf{B}_e - \mathbb{D}(\mathbf{B}_e)^\nabla\mathbf{B}_e,\\ \boldsymbol{\Psi}^{-1}\mathbf{B}_e =& \mathbf{I} - \zeta\mathbf{B}_e - \tau\mathbf{B}_e^\nabla\mathbf{B}_e.\end{aligned}$$

Substituting the approximation $\mathbf{B}_e = \boldsymbol{\Psi} + \boldsymbol{\Psi}_1$ in the right-hand of the last equality and keeping the dominant terms, we have

$$\boldsymbol{\Psi}^{-1}\mathbf{B}_e = \mathbf{I} - \zeta\boldsymbol{\Psi} - \tau\boldsymbol{\Psi}^\nabla\boldsymbol{\Psi}.$$

So $\mathbf{\Psi}^{-1}\mathbf{B}_e\mathbf{n} = \mathbf{n} - \zeta a_0^2\mathbf{n} - \tau a_0^2\mathbf{\Psi}^{\nabla}\mathbf{n}$, and the equation (2.32) becomes,

$$\mathbf{n} \times [\mu\tau(a_0^2 - a_0^{-1})\mathbf{\Psi}^{\nabla}\mathbf{n} - k\theta''(z)\mathbf{n}^{\perp} = 0].$$

That can be with further simplifications derived into equation (2.46b).

7.1.4. Find the critical value ζ_c

In §2.4.1, we want to find non-trivial values, after solving the linearized equations around the trivial solution, we find with the first boundary condition a set of solutions. But we need that they match the second boundary condition. We showed in §2.4.1, the existence of non-trivial solution is equivalent to ask that the determinant of the following matrix vanishes,

$$A = \begin{pmatrix} \sin(\sqrt{\frac{\zeta\mu}{a_0 k}}(a_0^3 - 1)L) & \sin^2(\sqrt{\frac{\zeta\mu}{a_0 k}}\frac{(a_0^3-1)L}{2}) \\ 4\sin^2(\sqrt{\frac{\zeta\mu}{a_0 k}}\frac{(a_0^3-1)L}{2}) & -\sin(\sqrt{\frac{\zeta\mu}{a_0 k}}(a_0^3 - 1)L) \end{pmatrix}$$

Let be $\gamma = \sqrt{\frac{\zeta\mu}{a_0 k}}\frac{(a_0^3-1)L}{2}$, then,

$$\det(A) = -(\sin(2\gamma)^2 + \sin(\gamma)^4) = -\sin(2\gamma)^2 - (1 - \cos(2\gamma))^2 = 2(\cos(\gamma) - 1).$$

To have zero we need, $\gamma = 2\pi n$, $n \in \mathbb{N}$. Leading to the condition (2.50).

7.2. Appendix chapter 4

7.2.1. Fredholm operator and Implicit function theorem

Definition 7.2.1. *A bounded linear operator $T\colon X \to Y$ is called Fredholm operator if,* $\dim\ker(T) < +\infty$ *and* $\dim\operatorname{coker}(T) < +\infty$.

With the cokernel $\operatorname{coker}(T) := Y/\operatorname{im}(T)$, meaning that the second condition is equivalent to say that the image of T has a finite codimension ($\operatorname{codim}(\operatorname{im}(T)) = \dim(Y) - \dim(\operatorname{im}(T))$).

The implicit function theorem is the following,

Theorem 7.1. *Let F a $\mathscr{C}^p$-map from U an open neighborhood of the point $(x_0, \alpha_c) \in X \times \Lambda$ to Y such as $F(x_0, \alpha) = 0$ and $\det(J) \neq 0$.*

Then there exists a unique $\mathscr{C}^p$ function ϕ from V, open neighborhood of α_c, to Y and Ω, open neighborhood of (x_0, α_c) (with $\Omega \subset U$) such as,

$$\forall (x,\lambda) \in X \times \Lambda, \quad ((x,\lambda) \in \Omega \text{ and } F(x,\lambda) = 0) \iff (\lambda \in V \text{ and } x = \phi(\lambda)).$$

7.2.2. Use the adjoint operator to find the range

We explain in this section the reason to use the adjoint operator to find the projector to the range of the operator. Let $\mathrm{L} : X \to Y$ be our operator and $y \in \mathrm{range(L)} \subseteq Y$. Then, there exists $x \in X$ such as $\mathrm{L}x = y$.
Now, we want to split the space Y as the direct sum of range(L) and range(L)$^\perp$. Because it is difficult to define the first subspace, we avoid this problem by defining the second subspace. $y \in \mathrm{range(L)}^\perp \iff \langle y, \mathrm{L}x\rangle = 0, \forall x \in X$. But $\langle y, \mathrm{L}x\rangle = \langle \mathrm{L}^* y, x\rangle = 0,\ \forall x \in X$. We conclude that $\mathrm{L}^* y = 0$, in other words, $y \in \ker(\mathrm{L}^*)$.
And once the structure of the kernel of L^* is found, we can define the projector to the range of L as follows,

$$\mathbf{P}_{\mathrm{range(L)}} = \mathbf{I} - \mathbf{P}_{\ker(\mathrm{L}^*)}.$$

7.2.3. Euler Beam computations

The scalar product for the projection leading to equation (4.7) is detailed. First, the equation (4.5) is recalled:

$$\lambda A\cos(\pi x) + w''(x,A,\lambda) + (\lambda+\pi^2)\Big[w(x,A,\lambda) - \frac{(A\cos(\pi x) + w(x,A,\lambda))^3}{6}\Big] = 0.$$

Then the scalar product $\Big\langle *,\ 2\cos(\pi x)\Big\rangle$ gives the following terms:

- $\Big\langle w'' + (\lambda+\pi^2)w,\ 2\cos(\pi x)\Big\rangle = \Big\langle F_0(w),\ 2\cos(\pi x)\Big\rangle = 0$, by definition of the adjoint kernel. F_0 is the linear operator corresponding to the linearization of F about the trivial solution.
- $\Big\langle \lambda A\cos(\pi x),\ 2\cos(\pi x)\Big\rangle = \lambda A$.
- $\Big\langle \frac{\lambda+\pi^2}{6}(A\cos(\pi x) + w)^3,\ 2\cos(\pi x)\Big\rangle = \frac{\lambda+\pi^2}{6}\int_0^1 (A\cos(\pi x) + w(x,A,\lambda))^3\cos(\pi x)dx$.

The last term can be developed:

$$\int_0^1 \Big(2A^3\cos(4\pi x)^4 + 6A^2\cos(\pi x)^3 w + 3A(1+\cos(\pi x))w^2 + 2w^3\cos(\pi x)\Big)dx.$$

Then, applying two times $\cos(\theta)^2 = \frac{1+\cos(2\theta)}{2}$, the first term gives:

$$\int_0^1 2A^3\cos(4\pi x)^4 dx = 2A^3\int_0^1 \Big(\frac{3}{8} + \cos(2\pi x) + \frac{\cos(4\pi x)}{8}\Big)dx = \frac{3A^3}{4}.$$

The second term is developed using the formula $\cos(\theta)^3 = \frac{3}{4}\cos(\theta) + \frac{1}{4}\cos(3\theta)$. The first part is proportional to the kernel and then orthogonal to w.

$$\int_0^1 6A^2\cos(\pi x)^3 w dx = \frac{3A^2}{2}\int_0^1 \cos(3\pi x) w dx.$$

Then the equation (4.7) is found collecting all the terms.

For the equation (4.6a) the previous result is used, indeed the equation (4.5) has to be projected to the Kernel of the operator:

$$\begin{aligned}
&\lambda A\cos(\pi x) + w'' + (\lambda+\pi^2)w - \frac{(\lambda+\pi^2}{6}\Big[A^3\big(\frac{3}{4}\cos(\pi x) + \frac{1}{4}\cos(3\pi x)\big)\\
&+ 3A^2\cos(\pi x)^2 w + 3A\cos(\pi x)w^2 + w^3\Big] - \lambda A\cos(\pi x) - \frac{\lambda+\pi^2}{6}\Big[3\frac{A^3}{4}\cos(\pi x)\\
&+ \int_0^1 \big(\frac{3}{2}A^2 w\cos(3\pi x) + 3Aw^2(1+\cos(2\pi x)) + 2w^3\cos(\pi x)\big)dx\cos(\pi x)\Big].
\end{aligned}$$

The simplification between the highlighted terms gives directly the equation (4.6a).

7.2.4. Proof of the generalized equivariant branching lemma

Proof. Since fixed-point subspaces are flow-invariant, we have $F(\mathbf{U},\lambda) \in \mathrm{Fix}(\Sigma)$ for all $\mathbf{U} \in \mathrm{Fix}(\Sigma)$. Since $\dim(\mathrm{Fix}(\Sigma)) = 1$, we also have $\mathbf{U} = s\mathbf{W}$, $\forall \mathbf{U} \in \mathrm{Fix}(\Sigma)$ and

$$F(s\mathbf{W},\lambda) = H(s,\lambda)\mathbf{W}, \tag{7.1}$$

where $H(s,\lambda)$ is a scalar function and s is a scalar that parameterizes the solution branch. Now, since $\mathrm{Fix}(\Gamma) = \{0\}$, there is the trivial solution $F(\mathbf{0},\lambda) = 0$. Corresponding to $s = 0$, so we must have $H(0,\lambda) = 0$. We can perform in equation (7.1) a Taylor expansion with

respect to s:

$$\begin{aligned} F(s\mathbf{W},\lambda) =& H(0,\lambda)\mathbf{W} + \frac{\partial H}{\partial s}|_{s=0} s\mathbf{W} + \frac{1}{2}\frac{\partial^2 h}{\partial s^2}|_{s=0} s^2\mathbf{W} + \mathrm{o}(s^2) \\ =& \frac{\partial H}{\partial s}|_{s=0} s\mathbf{W} + \frac{1}{2}\frac{\partial^2 h}{\partial s^2}|_{s=0} s^2\mathbf{W} + \mathrm{o}(s^2) \\ =& K(s,\lambda) + \mathrm{o}(s^2). \end{aligned}$$

And

$$\begin{aligned} K(0,\lambda_c)\mathbf{W} &= DF|_{(\mathbf{0},\zeta_c)}\mathbf{W} = 0, \\ \frac{\partial K}{\partial \lambda}(0,\lambda_c)\mathbf{W} &= DF_\lambda|_{(\mathbf{0},\lambda_c)}\mathbf{W} \neq 0. \end{aligned}$$

hold by assumption. Since $\mathbf{W} \neq \mathbf{0}$, we have $K(0,\lambda_c) = 0$ and $\frac{\partial K}{\partial \lambda}(0,\lambda_c) \neq 0$. So by the implicit function theorem 7.1, for s small and λ close to λ_c (but $\lambda > \lambda_c$), we can solve $K(s,\lambda) = 0$ to find the unique solution for λ as a function of s.
Since $\dim(\mathrm{Fix}(\Sigma)) = 1$, $\mathbf{W}$ is unique for a given Σ, up to a scaling. And the solution branch is unique too. □

7.3. Code (*Mathematica*)

7.3.1. *Mathematica* code (Ch2)

First we define the different operators needed, especially the operator between the objects such outer product, multiplication etc...

```
(* ************************************************************************** *)
(*Here, matrix is tensor of order 2, and tensor is tensor of order 4*)

(*outer product vector*)
tp[a_, b_] := TensorProduct[a, b];

(*product matrices*)
PMM[A_, B_] := Table[Sum[A[[i, j]]*B[[j, k]], {j, 1, 3}], {i, 1, 3}, {k, 1, 3}];

(*Article: outer product tensors*)
tP[A_, B_] := Table[A[[h, i]]*B[[j, k]], {h, 1, 3}, {j, 1, 3}, {i, 1, 3}, {k, 1, 3}];

(*Classic: outer product tensors*)
tP2[A_, B_] := Table[A[[h, i]]*B[[j, k]], {h, 1, 3}, {i, 1, 3}, {j, 1, 3}, {k, 1, 3}];

(*Product tensors*)
```

```
PTT[A_, B_] := Table[Sum[Sum[A[[h, i]][[j, k]]*B[[j, k]][[l, m]], {j, 1, 3}], {k, 1, 3}],
{h, 1, 3}, {i, 1, 3}, {l, 1, 3}, {m, 1, 3}];

(*Product tensor*Matrix*)
PTM[A_, B_] := Table[Sum[Sum[A[[h, i]][[j, k]]*B[[j, k]], {j, 1, 3}], {k, 1, 3}],
{h, 1, 3}, {i, 1, 3}];

(*Transpose of matrix*)
bTranspose[A_] :=Table[A[[j, i]], {i, 1, 3}, {j, 1, 3}];

(*Trace of a matrix*)
bTrace[A_] := Sum[A[[i, i]], {i, 1, 3}];

(*Scalar product matrices*)
Ps[A_, B_] := bTrace[PMM[bTranspose[B], A]];

(*Identity matrix*)
bI = IdentityMatrix[3];

(*Laplacian*)
Lap[f_] := D[f, {x, 2}] + D[f, {y, 2}] + D[f, {z, 2}] ;

(* Gradient of Matrix*)
bGradT[T_, coor_] := Table[D[T[[h, i]], {coor[[j]], 1}], {h, 1, 3}, {i, 1, 3},
{j, 1, 3}];

(*Apply the Gradient of a Matrix to a vector*)
bGradTV[Grd_, vec_] := Table[Sum[Grd[[h, i, j]]*vec[[j]], {j, 1, 3}], {h, 1, 3},
{i, 1, 3}];
(* ********************************************************************** *)
```

We define then the quantities: velocity field, shape tensor, Cauchy Tensor etc...

```
(* ********************************************************************** *)
(*Velocity field*)

bv = {vx[z], 0, 0};
(*Gradient of velocity*)
Dv = Grad[bv, {x, y, z}];
(*Sym and Skw parts of the gradient *)
```

```
bD = 1/2 (Dv + Transpose[Dv]);
bW = 1/2 (Dv - Transpose[Dv]);

Tr[bD];(*Must be zero*)

(*Director*)
bn = {Cos[th[z]], 0, Sin[th[z]]}; Dn = Grad[bn, {x, y, z}];
Ln = Lap[bn]; MatrixForm[Ln];

(*shape tensor and inverse*)
bPsi = a0^2 tp[bn, bn] + 1/a0 (bI - tp[bn, bn]) ;
bPsim = 1/a0^2 tp[bn, bn] + a0 (bI - tp[bn, bn]);

(*codeformational derivative of shape tensore*)
bPsiucd = D[bPsi, t] + bGradTV[bGradT[bPsi, {x, y, z}], bv]
- Dv . bPsi - bPsi . Transpose[Dv];

(*activity*)
bTa = -(1/2) rho mu zeta bI;
(*Psi^-1Be)
bPsimB = bI + 2/(rho mu)bTa . bPsi - tau bPsiucd . bPsi;

(*Cauchy tensor and molecular field*)
bT = -p[z] bI + rho mu (bPsimB - bI) - rho k Transpose[Dn] . Dn;
bh = -rho mu (1 - a0^-3) bPsimB . bn - rho k Ln;

(*Stokes equations*)
eq1 = Simplify[{D[bT[[1, 3]], z], D[bT[[2, 3]], z], D[bT[[3, 3]], z]}];
(*First equation*)
eq1[[3]]

(*Molecular field equation*)
eq2 = Simplify[Cross[bn, bh]]
(* ********************************************************************** *)
```

Now, we linearize the equations, using an expansion of the quantities v_x and θ with respect to ϵ (eps in the code). Then, the equations can be solved with one boundary conditions (here $z = 0$).

```
(* ********************************************************************** *)
```

```
(*Expansion of the quantities*)
soseps = {th[z] -> eps th1[z], th'[z] -> eps th1'[z], th''[z] -> eps th1''[z],
vx[z] -> eps v1[z], vx'[z] -> eps v1'[z], vx''[z] ->  eps v1''[z]};

(*Subsitute the expansions in the equations*)
eq1 = 4 (-1 + a0^3) (-2 a0 zeta Cos[2 th[z]] + 2 tau (1 + a0^3
+ (-1 + a0^3) Cos[2 th[z]]) Sin[2 th[z]] vx'[z]) th'[z]
- tau (-5 + 2 a0^3 - 5 a0^6 + 4 (-1 + a0^6) Cos[2 th[z]]
+ (-1 + a0^3)^2 Cos[4 th[z]]) (vx'')[z] //. soseps;

eq2 = (-1 + a0^3)mu tau (1 - a0^3 + (1 + a0^3) Cos[2 th[z]]) vx'[z]
+ 2 a0^2 k th''[z] //. soseps;

(*Expand the non-linear terms of the equations*)

eq1eps = Normal[Series[eq1, {eps, 0, 1}]]
eq2eps = Normal[Series[eq2, {eps, 0, 1}]]

(*Solve the linearized equations with the boundary condition at z=0*)
sol = DSolve[{eq1eps == 0, eq2eps == 0, v1[0] == 0, th1[0] == 0},
{v1[z], th1[z]}, z] // FullSimplify

(*Solutions*)
v[z_] := 1/((-1 + a0^3)mu tau) (-a0^2 k c1 (-1 +
Cos[((-1 + a0^3) z Sqrt[zeta] Sqrt[mu])/(Sqrt[a0] Sqrt[k])])
+ 1/Sqrt[zeta] Sqrt[a0] Sqrt[k] Sqrt[mu]tau
c2 Sin[((-1 + a0^3) z Sqrt[zeta] Sqrt[mu])/(Sqrt[a0] Sqrt[k])]);

th[z_] := 1/(a0 (-1 + a0^3) zeta) (tau c2 (-1 +
Cos[((-1 + a0^3) z Sqrt[zeta] Sqrt[mu])/(Sqrt[a0] Sqrt[k])])
+ 1/Sqrt[mu] a0^(3/2) Sqrt[k] Sqrt[zeta] c1
Sin[((-1 + a0^3) z Sqrt[zeta] Sqrt[mu])/(Sqrt[a0] Sqrt[k])]);

(*Satisfy the other boundary condition*)
v[L]
th[L]

(*Matrix A*vec(c)=0*)
A = {{-((a0^2 k)/((-1 + a0^3) mu tau)) (-1 +
```

```
Cos[((-1 + a0^3) L Sqrt[zeta] Sqrt[mu])/(Sqrt[a0] Sqrt[k])]),
((1/Sqrt[zeta]) Sqrt[a0] Sqrt[k]Sqrt[mu] tau )/((-1 + a0^3) mu tau)
Sin[((-1 + a0^3) L Sqrt[zeta] Sqrt[mu])/(Sqrt[a0] Sqrt[k])]},
{1/Sqrt[mu] a0^(3/2) Sqrt[k]Sqrt[zeta]
Sin[((-1 + a0^3) L Sqrt[zeta] Sqrt[mu])/(Sqrt[a0] Sqrt[k])]/(a0 (-1 + a0^3) zeta),
tau  (-1 + Cos[((-1 + a0^3) L Sqrt[zeta] Sqrt[mu])
/(Sqrt[a0] Sqrt[k])])/(a0 (-1 + a0^3) zeta)}};

FullSimplify[Det[A]]

(* Critical condition: Det[A]=0*)
Solve[((a0^3 - 1) L Sqrt[zeta] Sqrt[mu])/(Sqrt[a0] Sqrt[k]) == 2 n pi, k]
// FullSimplify


(*Solutions *)
th1[z_] = A1 Sin[(n pi z)/L]^2 + B1 Sin[(2 n pi z)/L];
v1[z_] = A2 Sin[(n pi z)/L]^2 + B2 Sin[(2 n  pi z)/L]
/. {B2 ->  (L a0 zeta (1 - a0^3)  )/(4 tau n pi) A1,
A2 -> (a0 (a0^3 - 1) L zeta)/(n pi tau) B1};

(*Give values to the parameters to plot the curves*)
(* ************************************************************************ *)
```

7.3.2. *Mathematica* code(Ch3)

For the computations of §3.2 and §3.3, the changes are simple, only the corresponding lines to the change have to be rewritten.

```
(* ************************************************************************ *)
(*In the quantities for changing the active tensor*)
bTa = -(1/2) rho mu zeta bPsi;

(*After computing the Cauchy tensor*)
(*no shear stress*)
Dot[bT, {0, 0, 1}] . {1, 0, 0} //. {z -> L, th[L] -> 0}

(*After solving the linear equations with the first boundary condition,
force this new one and compute the new matrix A.*)
(* ************************************************************************ *)
```

For the relaxations times it is a little longer, we have to write the base for the tensors $\mathbb{D}$ and $\mathbb{T}$. There are two options: the first consists to take the basis of $\mathbb{R}^3$ taking $\mathbf{e}_3 = \mathbf{n}$. With this base, build the basis of the symmetric tensors and express the two tensors. However, $\mathbb{T}$ is not symmetric with the scalar product associated with this basis. The second option is to project the previous basis into the space of symmetric tensors with a different scalar product which respects the symmetries of $\mathbb{T}$.

```
(* ********************************************************************** *)
(*OPTION 1: *)

(*Base of R^3*)
e1 = {Sin[th[z]], 0, -Cos[th[z]]};
e2 = {0, 1, 0};
(*e3=bn*)

(*Base of symmetric tensors space*)
E1 = 1/Sqrt[2] (tp[e2, bn] + tp[bn, e2]); E2 =
1/Sqrt[2] ( tp[e1, bn] + tp[bn, e1]);
E3 = 1/Sqrt[2] (  tp[e1, e2] +  tp[e2, e1]); E4 =
1/Sqrt[2] (tp[e1, e1] - tp[e2, e2]);
E5 = Sqrt[3]/Sqrt[2] ( tp[bn, bn] - 1/3 bI); E6 = 1/Sqrt[3] bI;

bTI = PTT[tP[bPsim, bPsim], tP[bPsi, bPsi]];

tau55 = taus + taud/(9 a0^3) ((4 a0^6 + a0^3 + 4) Cos[2*w] - Sqrt[2] (a0^3 - 1)^2 Sin[2*w]
tau56 = taud/(9 a0^3)((2 a0^6 + 8 a0^3 - 1) Sin[2*w] + 2 Sqrt[2] (a0^3 + 1-2 a0^6) Cos[2*
tau65 = taud/(9 a0^3) ((-a0^6 + 8 a0^3 + 2) Sin[2*w] + 2 Sqrt[2] (a0^6 + a0^3 - 2) Cos[2*
tau66 = taus + taud/(9 a0^3)(Sqrt[2] (a0^3 - 1)^2 Sin[2*w]-(4 a0^6 + a0^3 + 4) Cos[2*w]);

bTtau = tau1 tP2[E1, E1] + tau1 tP2[E2, E2] + tau2 tP2[E3, E3] + tau2 tP2[E4, E4] +
tau55 tP2[E5, E5] + tau56 tP2[E5, E6] + tau65 tP2[E6, E5] + tau66 tP2[E6, E6];


bDtau= PTT[tP[bPsim, bPsim], bTtau11];
bPsimB = bI + 2/(rho mu) bTa . bPsi - PTM[bDtau, bPsiucd] . bPsi;
(* ********************************************************************** *)

(*OPTION2: *)
```

```
L1 = Sqrt[a0] E1; L2 = Sqrt[a0] E2; L3 = 1/a0 E3; L4 = 1/a0 E4;
L5 = Sqrt[2/3] ( a0^2 tp[bn, bn] - 1/(2 a0) (bI - tp[bn, bn]));
L6 = 1/Sqrt[3] bPsi;
BL = {L1, L2, L3, L4, L5, L6};

bR = tP[bPsim, bPsim];

LtP[A_, B_] := Table[A[[p, q]]*Sum[Sum[B[[l, k]]*bR[[l, k]][[i, j]], {l, 1, 3}],
 {k, 1, 3}],{p, 1, 3}, {q, 1, 3}, {i, 1, 3}, {j, 1, 3}];
LPs[A_, B_] := bTrace[bTranspose[A] . (bPsim . B . bPsim)];

bTtau = Table[0, {i, 6}, {j, 6}];

bTtau[[1, 1]] = tau1; bTtau[[2, 2]] = tau1; bTtau[[3, 3]] = tau2;
bTtau[[4, 4]] = tau2; bTtau[[5, 5]] = taus + taud*Cos[2*w];
bTtau[[5, 6]] = taud*Sin[2*w]; bTtau[[6, 5]] = taud*Sin[2*w];
bTtau[[6, 6]] = taus - taud*Cos[2*w];

bTt= Table[0, {i, 3}, {j, 3}];

For[i = 1, i < 7, i++,
For[j = 1, j < 7, j++,
bTt = bTt + bTtau[[i, j]]*LtP[BL[[i]], BL[[j]]]]];

bDtau= PTT[tP[bPsim, bPsim], bTt21];
bPsimB = bI + 2/(\[Rho] \[Mu]) bTa . bPsi - PTM[bDtau, bPsiucd] . bPsi;

(*replace bPsimB in the definition of the Cauchy tensor and the molecular field
to get the new equation*)
(* ********************************************************************** *)
```

7.3.3. *Mathematica* code for Lyapunov-Schmidt reduction

First, we want to make dimensionless the equations and then, as we did in §4.3, we want an expansion of our equations and we choose to order 3.

```
(* ********************************************************************** *)
(*Dimensionless*)
F[v_, th_, zeta_] := {L *(4 (a0^3-1) (-2 a0 zeta Cos[2 th] + 2 tau (1 + a0^3
```

```
+ (-1 + a0^3) Cos[2 th]) Sin[2 th] D[v, {z, 1}]) D[th, {z,1}] - tau (-5
+ 2 a0^3 - 5 a0^6 + 4 (a0^6-1) Cos[2 th]
+ (-1 + a0^3)^2 Cos[4 th]) D[v, {z, 2}]),
L^2/(k)*(tau (-1 + a0^3)mu (1 - a0^3 + (1 + a0^3) Cos[2 th]) D[v, {z, 1}]
+ 2 a0^2 k D[th, {z, 2}])} /. {mu-> r k/L^2};

v[z_] = L/tau  V[z/L]; th[z_] = q[z/L];
F[v[z], th[z], zeta (1 + lamb)] //. {z -> L \[Xi]} // FullSimplify
(* ********************************************************************** *)
(*Expansion*)
equations = {8 (-1 + a0^3) q'[xi] (-a0 zeta (1 + lamb) Cos[2 q[xi]]
+ (1 + a0^3 + (-1 + a0^3) Cos[2 q[xi]]) Sin[2 q[xi]] V'[xi])
+ (5 - 2 a0^3 + 5 a0^6 - 4 (-1 + a0^6) Cos[2 q[xi]]
- (-1 + a0^3)^2 Cos[4 q[xi]]) V''[xi],
(-1 + a0^3) r (1 - a0^3 + (1 + a0^3) Cos[2 q[xi]]) V'[xi] + 2 a0^2 q''[xi]};
bF= Normal[Series[equations, {q[xi], 0, 3}]];

(* ********************************************************************** *)
```

Before to perform the Lyapunov-Schmidt reduction, we find the kernels of the linear operator and its adjoint. We define also the projectors to the orthogonal of the adjoint kernel, corresponding to equation (4.20), the projector to the adjoint kernel, corresponding to equation (4.21), and the projector to the kernel of the linear operator.

```
(* ********************************************************************** *)
soslin = {zeta -> a/(8 a0 (-1 + a0^3) ), r -> b/(2 (-1 + a0^3)),
a0^2 -> c/2};
sosinv = {a -> zeta (8 a0 (-1 + a0^3) ), b -> r (2 (-1 + a0^3)),
c -> 2 a0^2};

(*Linear equations*)
Normal[Series[equations, {q[xi], 0, 1}]];
eqlin = {-8 a0 (-1 + a0^3) zeta q'[xi] + 8 V''[xi],
2 (-1 + a0^3) r V'[xi] + 2 a0^2 q''[xi]} //. soslin
solin = Flatten[DSolve[{eqlin == {0, 0}, V[0] == 0, q[0] == 0},
{V[xi], q[xi]}, xi]];
(* ********************************************************************** *)
(*Bounday conditions at xi = 1*)
```

```
{(q[xi] /. solin /. {xi -> 1}), (V[xi] /. solin /. {xi -> 1})}
(*Transform the boundary condition into A*vec(c)=0*)
A = {{(2 (-4 Sqrt[b]+4 Sqrt[b] Cos[(Sqrt[a] Sqrt[b])
/(2 Sqrt[2] Sqrt[c])]))/(a Sqrt[b]),
 (2 (Sqrt[2] Sqrt[a] Sqrt[c]Sin[(Sqrt[a] Sqrt[b])
 /(2 Sqrt[2] Sqrt[c])]))/(a Sqrt[b])},
 {(2 Sqrt[2] Sqrt[b] Sqrt[c]Sin[(Sqrt[a] Sqrt[b])
  /(2 Sqrt[2] Sqrt[c])])/(Sqrt[a] b),
  (Sqrt[a] c - Sqrt[a] c  Cos[(Sqrt[a] Sqrt[b])
  /(2 Sqrt[2] Sqrt[c])])/(Sqrt[a] b)}};

(*We want Det[A]=0*)
(* ************************************************************************ *)
(*Solutions*)
TrigReduce[solin /.Flatten[
Solve[{(Sqrt[a] Sqrt[b])/(4 Sqrt[2] Sqrt[c]) ==  pi}, {a}]] //FullSimplify] /. sosinv
Flatten[Solve[{(Sqrt[a] Sqrt[b])/(4 Sqrt[2] Sqrt[c]) ==  pi}
/. {a -> zeta (8 a0 (-1 + a0^3) ), b -> r (2 (-1 + a0^3)), c -> 2 a0^2}, {zeta}]]

(* ************************************************************************ *)
(*For the adjuent only change the equations and after applying
the boundary condition, change A*)

eqadj = {8 V''[xi] - 2 (-1 + a0^3) r q'[xi],
8 a0 (-1 + a0^3) zeta V'[xi] + 2 a0^2 q''[xi]} /. soslin
(* ************************************************************************ *)
(*Vectors of the Kernels of L and its adjoint*)

u1v[xi_] = (1 - Cos[2 pi xi]); u2v[xi_] =  Sin[2 pi xi];
u1q[xi_] = ((-1 + a0^3)  r )/(2 pi (a0^2) )Sin[2 pi xi];
u2q[xi_] = ((-1 + a0^3)  r )/(2 pi (a0^2))( Cos[2 pi xi] - 1);
u1 = {u1v[xi], u1q[xi]}; u2 = {u2v[xi], u2q[xi]};

uadj1 = {(8 pi (1 - Cos[2 pi xi]))/((-1 + a0^3) r), Sin[2 pi xi]} // FullSimplify;
uadj2 = {(8 pi  Sin[2 pi xi])/((-1 + a0^3) r),(Cos[2 pi xi] - 1)} // FullSimplify;

(*Norm of the adjoint vectors*)
nor1 = Simplify[Sqrt[Integrate[Dot[uadj1, uadj1], {xi, 0, 1}]]];
nor2 = Simplify[Sqrt[Integrate[Dot[uadj2, uadj2], {xi, 0, 1}]]];
```

```
(*Projector to the orthgonal of the adjoint kernel *)
Qadj[{a_, b_}] := Simplify[{Integrate[{a, b} . uadj1/nor1, {xi, 0, 1}],
Integrate[{a, b} . uadj2/nor2, {xi, 0, 1}]}];
ImQadj[{a_, b_}] := Simplify[{a, b} -
1/nor1 Integrate[{a, b} . uadj1/nor1, {xi, 0, 1}] uadj1 -
1/nor2 Integrate[{a, b} . uadj2/nor2, {xi, 0, 1}] uadj2];

(*Projector to the linear kernel*)
Projlin[{a_, b_}] := {Simplify[Integrate[{a, b} . u1/noru1, {xi, 0, 1}]],
Simplify[Integrate[{a, b} . u2/noru2, {xi, 0, 1}]]};

(*Transform the equations with respect to the critical value of zeta*)
bF=bF./{zeta-> (4 a0 pi^2)/((-1 + a0^3)^2 r)}//FullSimplify;

(*Expansion of the solution for LS reduction*)

V[xi_] := al u1v[xi] + bet u2v[xi] + wv[xi];
q[xi_] := al u1q[xi] + bet u2q[xi] + wq[xi];

sosper = {al -> eps al, bet -> eps bet, wv -> Function[{xi}, eps^2 wv[xi]],
wq -> Function[{xi}, eps^2 wq[xi]], lamb -> eps lamb};
(*Assume that w is order two at least in alpha and beta,
we keep only term of order 3*)
eqw = Collect[ Normal[Series[bF /. sosper, {eps, 0, 3}]] /. eps -> 1,
{al, bet, lamb}, FullSimplify]
(* ********************************************************************** *)
```

From now, we will not write the equations even if they were in the code because they are too long and it is irrelevant. If the reader wants to check, he is invited to go on the Github link where he will find the complete code.
From the previous code, we get two equations but we have to perform a supplement dominant balance argument because the program is not able to compare λw with the power of α and β. So, we put these terms to zero by hand.
Our first approach is to solve directly the equations thanks to the program. And then ask for the supplement boundary condition and the orthogonality with the linear kernel. This allows us to see the form of the solution but also to have a result for the bifurcation diagram (see equations (4.22a) and (4.22b)) which can be confirmed by the Lyapunov-Schmidt reduction. An interesting remark, the bifurcation equation is get when applying

the second boundary condition while forcing the orthogonality allows us to get the unicity of the solution by fixing the constants of integration.

```
(* ********************************************************************** *)
(*Solve equations*)
sol = Flatten[DSolve[{eqw1 == {0, 0}, wq[0] == 0, wv[0] == 0},
{wq[xi], wv[xi]}, xi] //TrigReduce];

(*Impose orthogonality*)
ccsos = Flatten[Solve[Projlin[{wv[xi] /. sol, wq[xi] /. sol}] == 0, {c1, c2}]];
(*See the form of the solution)
Collect[sol, {xi, Sin[a_], Cos[a_]}, FullSimplify]

(*Impose the second boundary condition*)
wv[xi] /. sol /. ccsos /. {xi -> 1} // FullSimplify;
wq[xi] /. sol /. ccsos /. {xi -> 1} // FullSimplify;

(*Here we get the bifurcation equation*)
(* ********************************************************************** *)
```

Thereby, we can make an ansatz on the form of $\mathbf{w}$. We impose on the ansatz to be orthogonal to the kernel of the linear operator and to satisfy the boundary conditions. These constraints allow us to impose some equations between the constants of the ansatz. Then, we apply the two operators. First the projector to the orthogonal of the adjoint kernel to get equation (4.20). All the constants of the ansatz are fixed, we substitute the solution in the general equation and we perform the second projection to the adjoint kernel to obtain the bifurcation equation (4.21).

```
(* ********************************************************************** *)
wov[xi_] = K1 u1v[xi] + K2 u2v[xi];
woq[xi_] = K1 u1q[xi] + K2 u2q[xi];

wv[xi_] = wov[xi] + xi (F0 + F1 Cos[2 pi xi] + F2 Sin[2 pi xi]) +
Sum[Ak (1 - Cos[2 k pi xi]), {k, 1, 3}] + Sum[Bk Sin[2 k pi xi], {k, 1, 3}];
wq[xi_] = woq[xi] + xi (G, 0] + G1 Cos[2 pi xi] + G2 Sin[2 pi xi]) +
Sum[Ck (1 - Cos[2 k pi xi]), {k, 1, 3}] + Sum[Dk Sin[2 k pi xi], {k, 1, 3}];

coefficients =
Join[Table[Ak, {k, 1, 3}], Table[Bk, {k, 1, 3}], Table[Ck, {k, 1, 3}],
```

```
Table[Dk, {k, 1, 3}], Table[Fk, {k, 0, 2}], Table[Gk, {k, 0, 2}], {K1, K2}];

(*Boundary conditions*)
sosc = Flatten[Solve[{wv[1], wq[1]} == {0, 0}]];

(*Orthogonality with the kernel*)

ort = Flatten[Solve[Projlin[{wv[xi] /. sosc, wq[xi] /. sosc}] ==
 {0, 0},coefficients]] //Simplify;
sosc = Join[sosc /. ort, ort]

(* ************************************************************************ *)
(*First projection to the orthogonal of the kernel*)
outeq = Collect[ImQadj[(eqw/.sosc)], {Sin[a_], Cos[a_]}, Simplify]
flist = Join[{xi Cos[2 pi xi], xi Sin[2 pi xi]}, Table[Cos[2 k pi xi], {k, 1, 3}],
Table[Sin[2 k pi xi], {k, 1, 3}]];

eqcoeff = Flatten[Map[Coefficient[outeq, #] &, flist] // FullSimplify];
sosc1 = Flatten[Solve[eqcoeff == 0, coefficients]];
sosc = Join[sosc /. sosc1, sosc1];

(*Second projection*)
Qeq = Collect[Qadj[eqw /. sosc], {Sin[a_], Cos[a_]}, Simplify];
flist = Join[Table[Cos[2 k pi xi], {k, 1, 1}],
Table[Sin[2 k pi xi], {k, 1, 1}]];
proj2 = Flatten[Map[Coefficient[Qeq, #] &, flist] // FullSimplify]
Solve[proj2 == 0, {al, bet}] /. {b -> 1, a0 -> 2}

(*Here we get the bifurcation equations*)
(* ************************************************************************ *)
```

Bibliography

[1] H. R. Brand, H. Pleiner, and D. Svenšek. Reversible and dissipative macroscopic contributions to the stress tensor: Active or passive? *The European Physical Journal E*, 37(9):1–10, 2014.

[2] C. Clapham, J. Nicholson, and J. R. Nicholson. *The concise Oxford dictionary of mathematics*. Oxford University Press, 2014.

[3] A. Doostmohammadi, J. Ignés-Mullol, J. M. Yeomans, and F. Sagués. Active nematics. *Nature Communications*, 9(1):3246, 2018. doi: 10.1038/s41467-018-05666-8. URL `https://doi.org/10.1038/s41467-018-05666-8`.

[4] S. A. Edwards and J. M. Yeomans. Spontaneous flow states in active nematics: A unified picture. *EPL (Europhysics Letters)*, 85(1):18008, jan 2009.

[5] Y. Fu, H. Yu, X. Zhang, P. Malgaretti, V. Kishore, and W. Wang. Microscopic swarms: From active matter physics to biomedical and environmental applications. *Micromachines*, 13(2):295, 2022.

[6] A. Ghosh, W. Xu, N. Gupta, and D. H. Gracias. Active matter therapeutics. *Nano Today*, 31:100836, 2020.

[7] R. Hoyle and R. B. Hoyle. *Pattern formation: an introduction to methods*. Cambridge University Press, 2006.

[8] F. C. Keber, E. Loiseau, T. Sanchez, S. J. DeCamp, L. Giomi, M. J. Bowick, M. C. Marchetti, Z. Dogic, and A. R. Bausch. Topology and dynamics of active nematic vesicles. *Science*, 345(6201):1135–1139, 2014.

[9] M. C. Marchetti, J. F. Joanny, S. Ramaswamy, T. B. Liverpool, J. Prost, M. Rao, and R. A. Simha. Hydrodynamics of soft active matter. *Rev. Mod. Phys.*, 85:1143–1189, Jul 2013.

[10] D. Marenduzzo, E. Orlandini, M. Cates, and J. Yeomans. Steady-state hydrodynamic instabilities of active liquid crystals: Hybrid lattice boltzmann simulations. *Physical Review E*, 76(3):031921, 2007.

[11] G. Popkin. The physics of life. *Nature*, 529(7584):16–18, 2016.

[12] J. Prost, F. Jülicher, and J.-F. Joanny. Active gel physics. *Nature Physics*, 11(2): 111–117, 2015. doi: 10.1038/nphys3224.

[13] H. R. Richard and D. Armbruster. Perturbation methods, bifurcation theory and computer algebra. *Applied Mathematical Sciences*, 1987.

[14] V. Schaller, C. Weber, C. Semmrich, E. Frey, and A. R. Bausch. Polar patterns of driven filaments. *Nature*, 467(7311):73–77, 2010.

[15] I. W. Stewart. *The static and dynamic continuum theory of liquid crystals: a mathematical introduction*. Crc Press, 2019.

[16] S. S. Turzi. Viscoelastic nematodynamics. *Phys. Rev. E*, 94:062705, Dec 2016.

[17] S. S. Turzi. Active nematic gels as active relaxing solids. *Phys. Rev. E*, 96:052603, Nov 2017.

[18] T. Vicsek, A. Czirók, E. Ben-Jacob, I. Cohen, and O. Shochet. Novel type of phase transition in a system of self-driven particles. *Physical review letters*, 75(6):1226, 1995.

[19] R. Voituriez, J.-F. Joanny, and J. Prost. Spontaneous flow transition in active polar gels. *EPL (Europhysics Letters)*, 70(3):404, 2005.

[20] J. M. Yeomans. The hydrodynamics of active systems. *La Rivista del Nuovo Cimento*, 40(1):1–31, Dec 2016.